

Supplementary Information

Phage-assisted evolution of botulinum neurotoxin proteases with reprogrammed specificity

Travis R. Blum^{1,2,3}, Hao Liu⁴, Michael S. Packer^{1,2,3}, Xiaozhe Xiong⁴, Pyung-Gang Lee⁴, Sicai Zhang⁴, Michelle Richter^{1,2,3}, George Minasov⁵, Karla J. F. Satchell⁵, Min Dong^{4*}, and David R. Liu^{1,2,3*}

¹Merkin Institute of Transformative Technologies in Healthcare, Broad Institute of Harvard and MIT, Cambridge, MA, 02142

²Department of Chemistry and Chemical Biology, Harvard University, Cambridge, MA, 02138

³Howard Hughes Medical Institute, Harvard University, Cambridge, MA, 02138

⁴Department of Urology, Boston Children's Hospital, Department of Microbiology and Department of Surgery, Harvard Medical School, Boston, MA, 02115

⁵Department of Microbiology-Immunology, Northwestern University School of Medicine, Chicago, IL 60611

Supplementary Figures S1-S25

Supplementary Tables 1-9

Supplementary Methods

Supplementary References

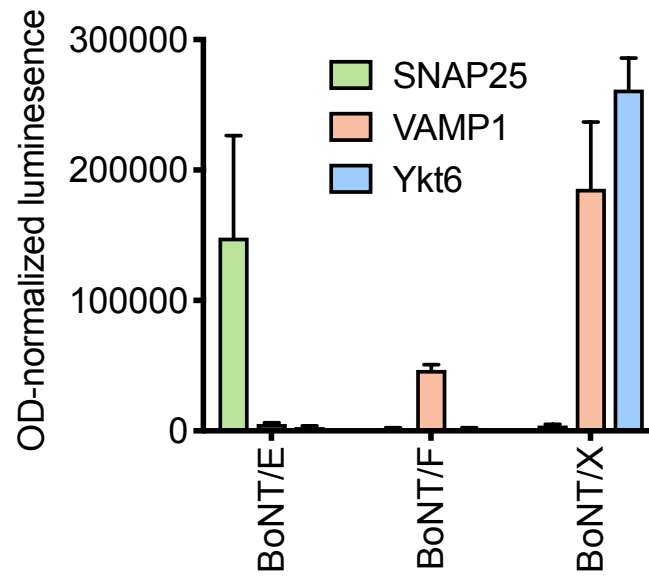


Figure S1. Validation of native activity for BoNT/E, BoNT/F, and BoNT/X proteases on a selection of their cognate SNARE targets *via* bacterial luciferase assay. Error bars represent the standard deviation of three biological replicates.

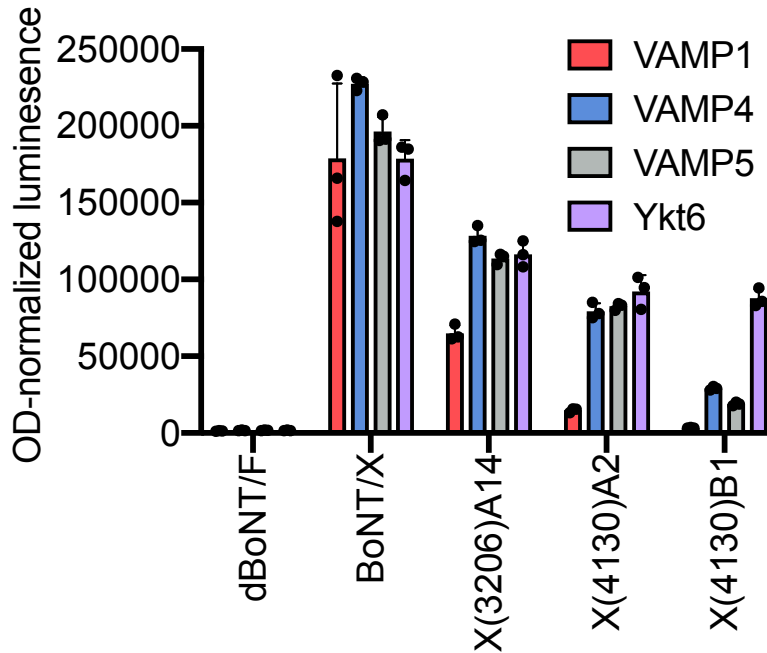


Figure S2. Apparent protease activity by luciferase assay of selected BoNT/X LC variants during the evolution of selective Ykt6-cleavage activity. dBoNT/F is an inactive BoNT/F protease mutant used as a negative control. Error bars represent the standard deviation of three biological replicates.

Passage number	Replicate A input phage dilution factor				Replicate B input phage dilution factor				Replicate C input phage dilution factor			
	Low stringency	Moderate stringency	High stringency	Very high stringency	Low stringency	Moderate stringency	High stringency	Very high stringency	Low stringency	Moderate stringency	High stringency	Very high stringency
1	100	100	100	100	100	100	100	100	100	100	100	100
2	100	100	100	100	100	100	100	100	100	100	100	100
3	100	100	100	100	100	100	100	100	100	100	100	100
4	100	100	100	100	100	100	100	100	100	100	100	100
5	100	100	100	100	100	100	100	100	100	100	100	100
6	400	400	400	400	400	400	400	400	400	400	400	400
7	400	400	400	400	400	400	400	400	400	400	400	400
8	1000	1000	1000	1000	1000	1000	1000	1000	1000	1000	1000	1000
9	1000	1000	1000	1000	1000	1000	1000	1000	1000	1000	1000	1000
10	1000	1000	1000	1000	1000	1000	1000	1000	1000	1000	1000	1000
11	1000	1000	1000	1000	1000	1000	1000	1000	1000	1000	1000	1000
12	250	250	250	250	250	250	250	250	250	250	250	250
13	2000	2000	2000	2000	2000	2000	2000	2000	2000	2000	2000	2000
14	2000	2000	2000	2000	2000	2000	2000	2000	2000	2000	2000	2000
15	5000	5000	5000	5000	5000	5000	5000	5000	5000	5000	5000	5000

	Positive selection AP	Negative selection AP
Very high stringency	AP _{T3} -Ykt6	AP _{neg} -VAMP1a
High stringency	AP _{T3} -Ykt6	AP _{neg} -VAMP1b
Moderate stringency	AP _{T3} -Ykt6	AP _{neg} -VAMP1c
Low stringency	AP _{T3} -Ykt6	AP _{neg} -VAMP1d

10² pfu/mL  10⁹ pfu/mL

Figure S3. Phage passage schedule for X(4130) protease evolution in PANCE using the dual positive and negative selection. The numbers in each cell indicate the dilution factor for the input phage population, while the shading indicates the output titer on the scale at the bottom. Blue outlines indicate populations that were used to inoculate subsequent passages, identified with blue text. Populations sequenced at the end of the PANCE campaign are indicated in orange text. Populations were only mixed within replicates, not between replicates.

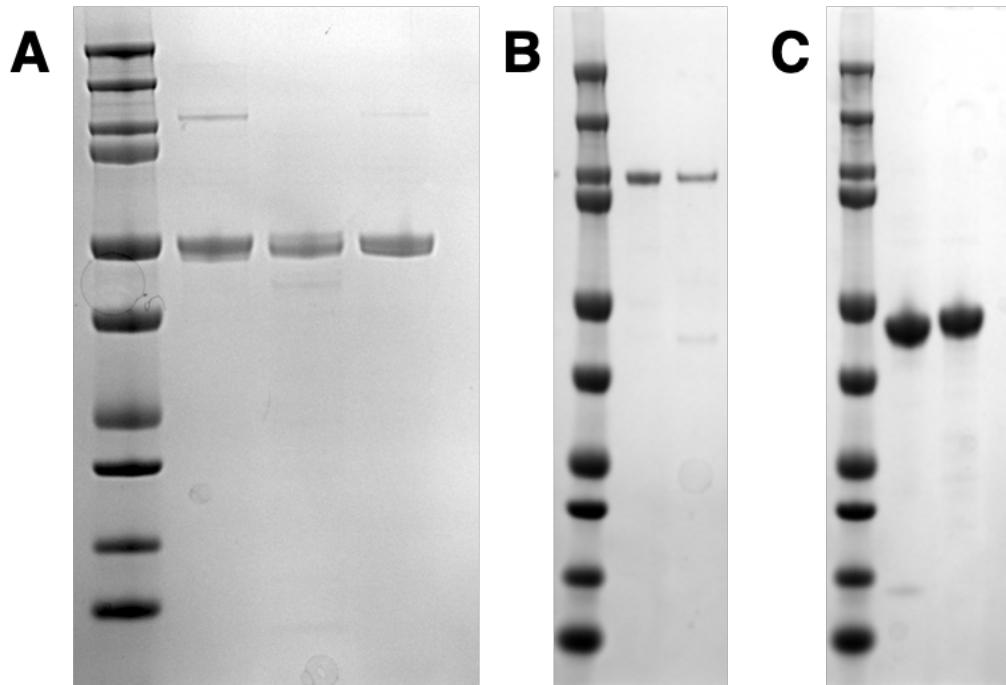


Figure S4: SDS-PAGE analysis of purified proteases used in this work. For purification strategies, see Materials and Methods. **(A)** Lane 1: BioRad Precision Plus Protein Standard; lane 2: wild-type BoNT/X LC; lane 3: BoNT/X(4130)B1 protease; lane 4: BoNT/X(5010)B1 protease. **(B)** Lane 1: BioRad Precision Plus Protein Standard; lane 2: MBP–BoNT/F LC; lane 3: MBP–BoNT/F(3230)A3 protease. **(C)** Lane 1: BioRad Precision Plus Protein Standard; lane 2: wild-type BoNT/E LC; lane 3: BoNT/E(4130)A2 protease. Gels were stained with GelCode™ Blue Stain Reagent (ThermoFisher 24590) and imaged with a G:Box Chemi XRQ (Syngene)

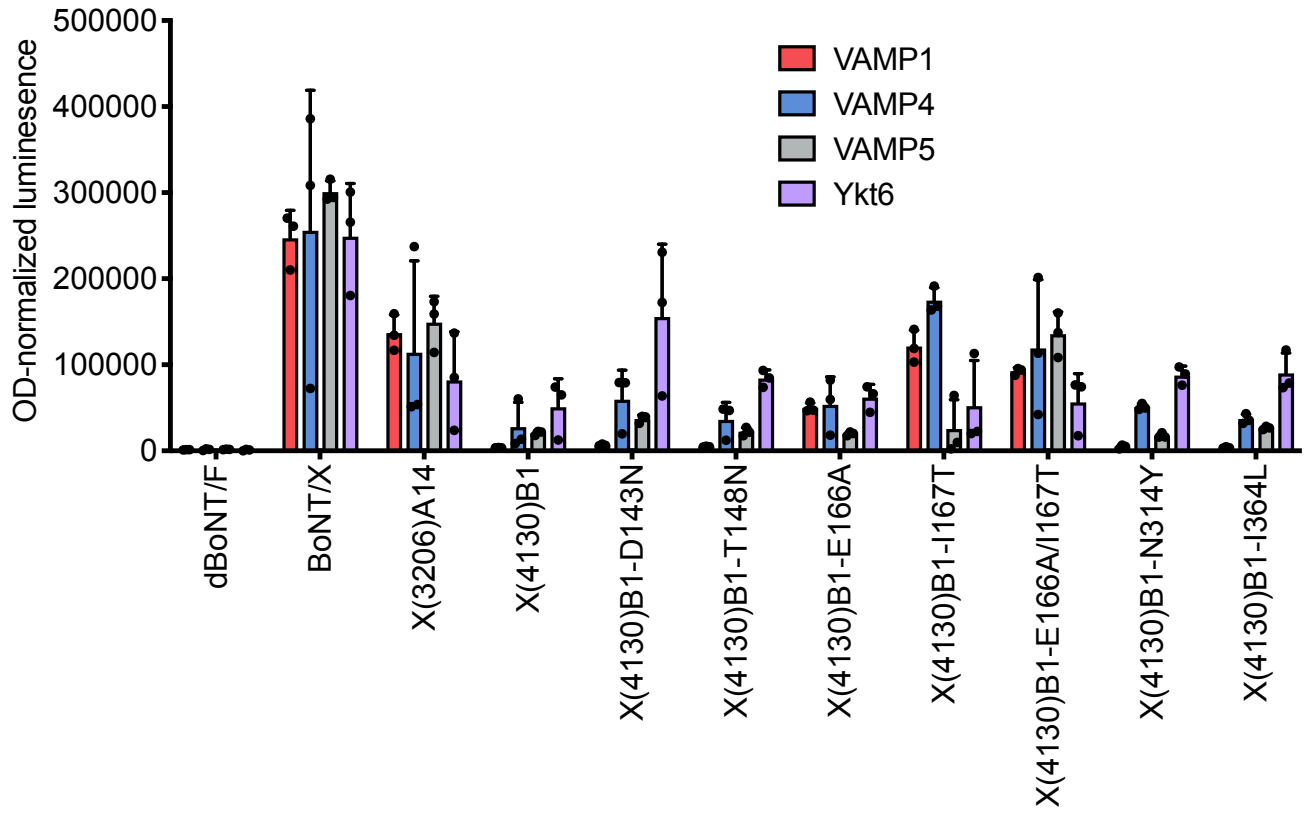


Figure S5: Luciferase activity assay of reversion mutants of X(4130)B1 protease on VAMP1, VAMP4, VAMP5, and Ykt6 T7-PAPs. dBoNT/F is an inactive BoNT/F protease mutant used as a negative control. Values and error bars represent the mean and standard deviation of three independent biological replicates

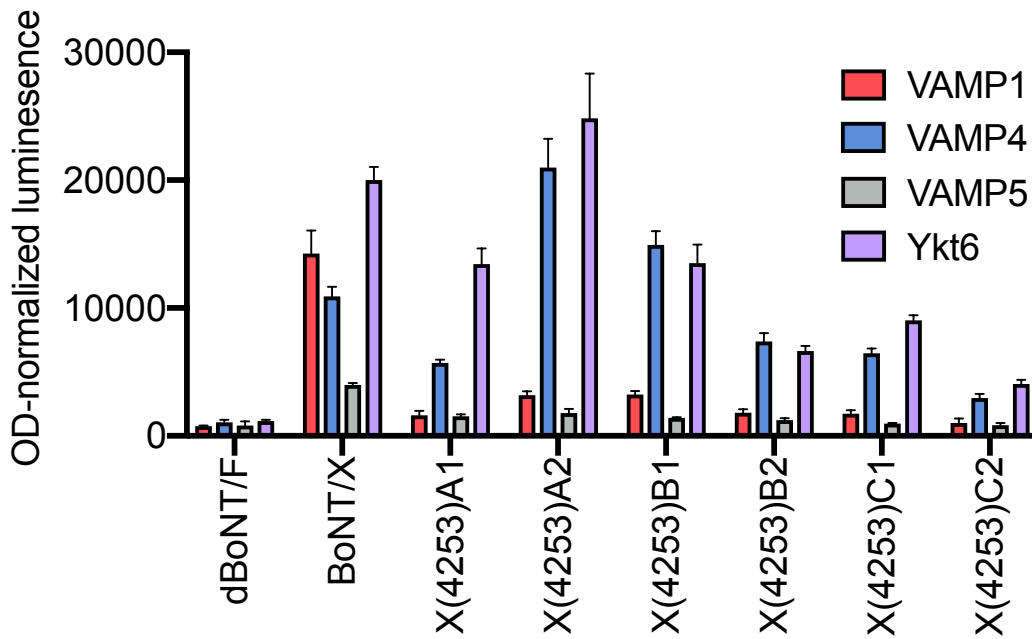


Figure S6. Luciferase assay to assess evolved BoNT/X protease variants after eight passages of dual positive- and negative-selection PANCE, with positive selection for VAMP4 cleavage and negative selection against VAMP1 cleavage. dBoNT/F is an inactive BoNT/F protease mutant used as a negative control. Values and error bars represent the mean and standard deviation of three technical replicates.

Passage number	Replicate A input phage dilution factor				Replicate B input phage dilution factor				Replicate C input phage dilution factor			
	Low stringency	Moderate stringency	High stringency	Very high stringency	Low stringency	Moderate stringency	High stringency	Very high stringency	Low stringency	Moderate stringency	High stringency	Very high stringency
1	100	100	100	100	100	100	100	100	100	100	100	100
2	100	100	100	100	100	100	100	100	100	100	100	100
3	100	100	100	100	100	100	100	100	100	100	100	100
4	100	100	100	100	100	100	100	100	100	100	100	100
5	200	200	200	200	200	200	200	200	200	200	200	200
6	200	200	200	200	200	200	200	200	200	200	200	200
7	500	500	500	500	500	500	500	500	500	500	500	500
8	500	500	500	500	500	500	500	500	500	500	500	500
9	200	200	200	200	200	200	200	200	200	200	200	200
10	1000	1000	1000	1000	1000	1000	1000	1000	1000	1000	1000	1000
11	1000	1000	1000	1000	1000	1000	1000	1000	1000	1000	1000	1000
12	5000	5000	5000	5000	5000	5000	5000	5000	5000	5000	5000	5000

	Positive selection AP	Negative selection AP
Low stringency	AP _{T3} -VAMP4	AP _{neg} -VAMP1a
Moderate stringency	AP _{T3} -VAMP4	AP _{neg} -VAMP1b
High stringency	AP _{T3} -VAMP4	AP _{neg} -VAMP1c
Very high stringency	AP _{T3} -VAMP4	AP _{neg} -VAMP1d

10² pfu/mL 10⁹ pfu/mL

Figure S7. Phage passage schedule for X(5010) protease evolution in PANCE using the dual positive and negative selection. The numbers in each cell indicate the dilution factor for the input phage population, while the shading indicates the output titer on the scale at the bottom. Purple outlines indicate populations that were used to inoculate subsequent passages, identified with purple text. Populations sequenced at the end of the PANCE campaign are indicated in orange text. Populations were only mixed within replicates, not between replicates.

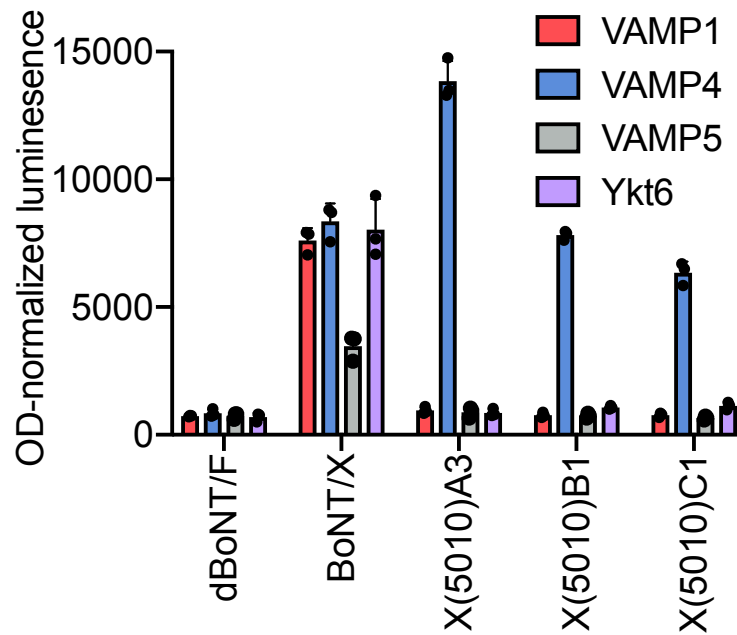


Figure S8. Luciferase assay to assess evolved BoNT/X protease variants after the final 12 passages of dual positive- and negative-selection PANCE, with positive selection for VAMP4 cleavage and negative selection against VAMP1 cleavage. dBoNT/F is an inactive BoNT/F protease mutant used as a negative control. Values and error bars represent the mean and standard deviation of three biological replicates.

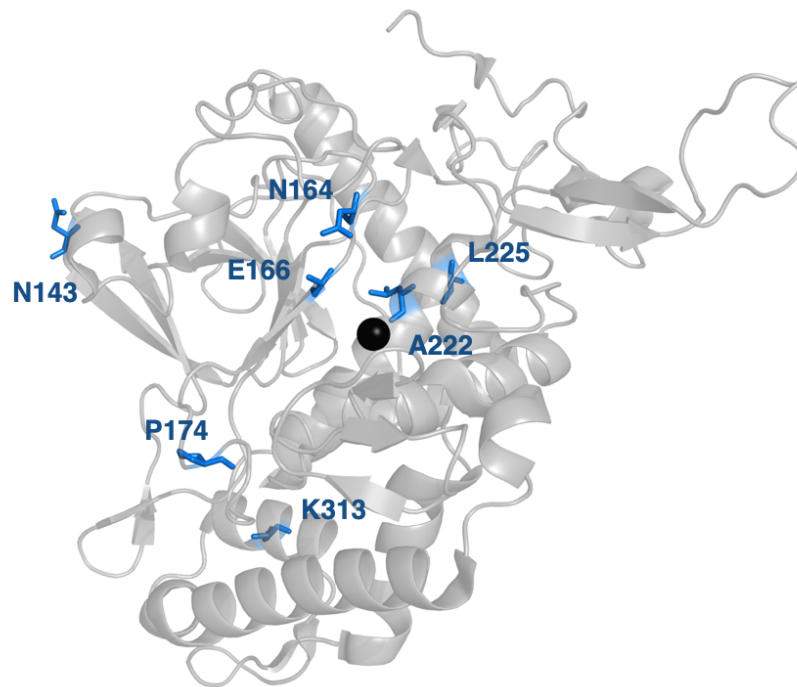


Figure S9. Annotated structure of BoNT/X protease (PDB 6F4E) showing the location of residues mutated in X(5010)B1 protease. Mutated residues are shown as blue sticks, and the active site zinc metallocofactor is shown as a black sphere.

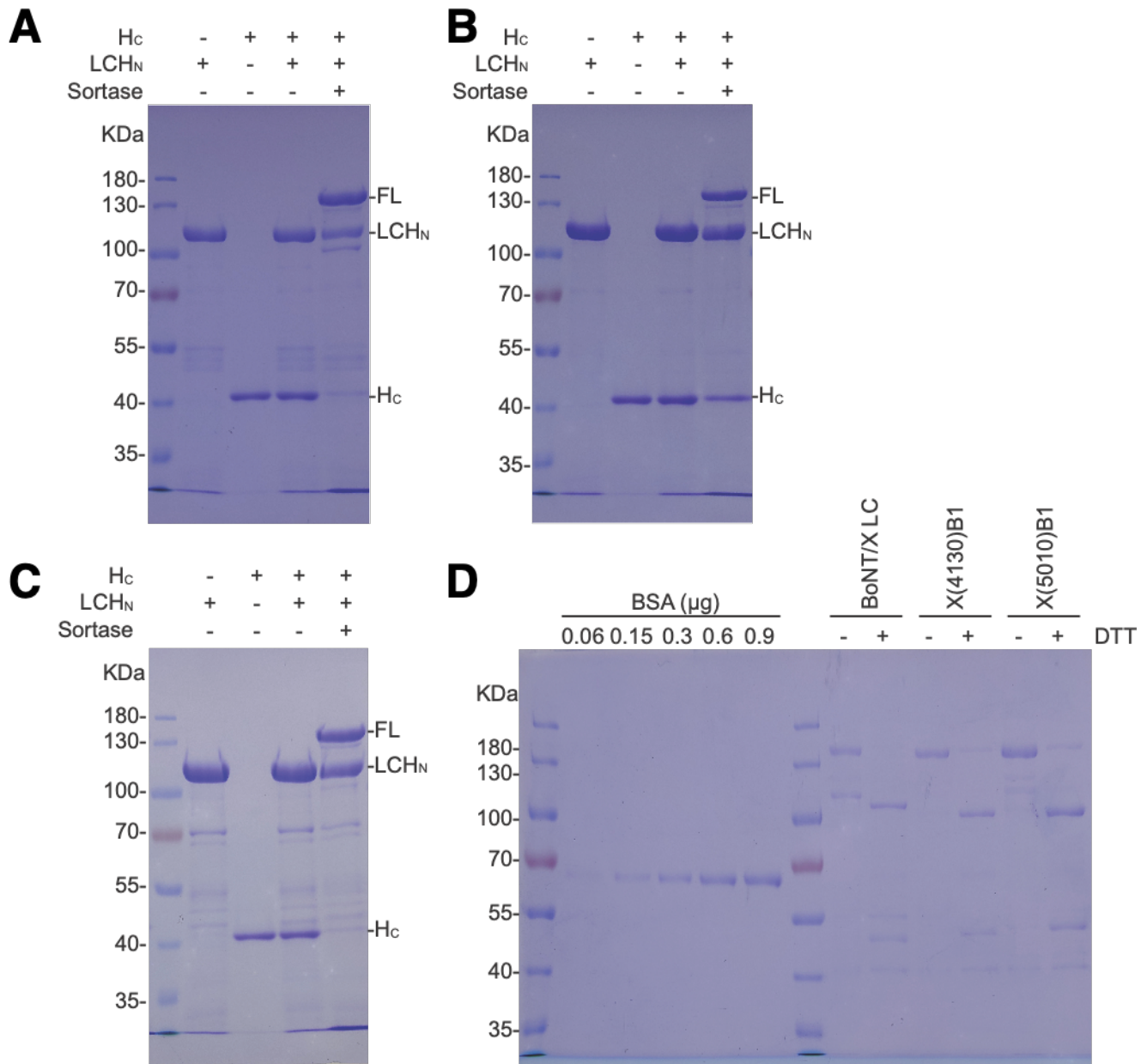


Figure S10. Sortase-mediated protein conjugation reactions to generate chimeric BoNT holotoxins using the LC and translocation domain (H_N) of BoNT/X (LCH_N) and the receptor-binding domain (H_C) of BoNT/A, with the LCs derived from (A) wild-type BoNT/X LC protease, (B) X(4130)B1, or (C) X(5010)B1. Sortase reaction mixtures were analyzed by SDS-PAGE and Coomassie blue staining. A thrombin cleavage site was introduced between the LC and H_N to facilitate toxin activation using thrombin. FL, full-length holotoxin. (D) Thrombin-activated full-length toxins with or without disulfide reduction by DTT were analyzed by SDS-PAGE and Coomassie blue staining. BSA is used as the standard to quantify full-length toxin.

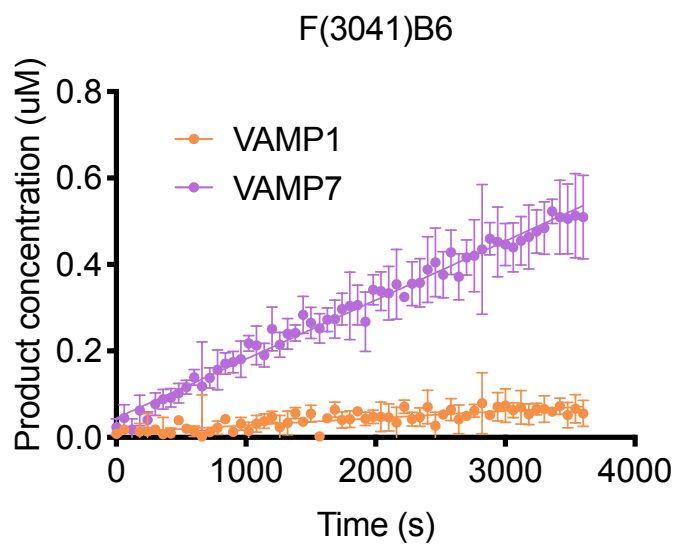


Figure S11. Comparison of evolved F(3041)B6 protease activity on VAMP1 and VAMP7. Reactions were performed using 50 nM protease with 5 mM substrate in 50 mM HEPES pH 7.3, 5 mM NaCl, 0.1% Tween-80, 2 mM DTT, 10 μM Zn(OAc)₂. Values and error bars represent the mean and standard deviation of three independent replicates.

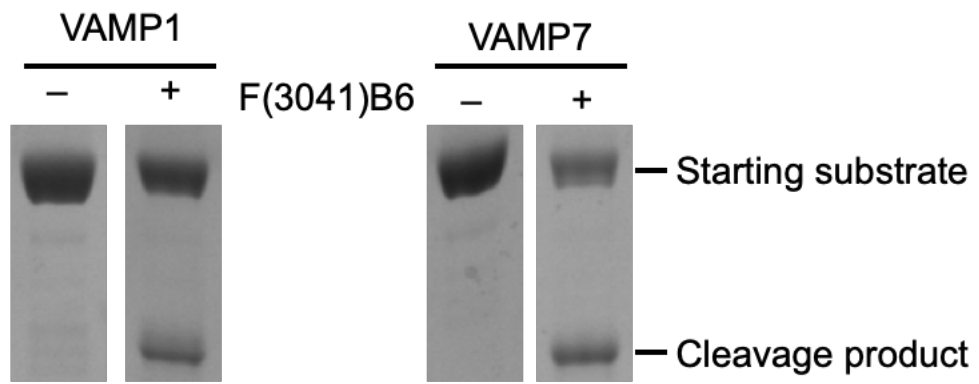


Figure S12. Proteolytic activity of F(3041)B6 on VAMP1(T29–K89) and VAMP7(K121–R180). Standard assay conditions used 5 mM substrate and 50 nM mF(3041)B6 for 1 h.

Replicate A input phage dilution factor					Replicate B input phage dilution factor				
Passage number	Low stringency	Moderate stringency	High stringency	Very high stringency	Passage number	Low stringency	Moderate stringency	High stringency	Very high stringency
1	50	50	50	50	1	50	50	50	50
2	100	100	100	100	2	100	100	100	100
3	100	100	100	100	3	200	100	100	100
4	200	200	200	200	4	200	200	200	200
5	200	200	200	200	5	200	200	200	200
6	200	200	200	200	6	200	200	200	200
7	200	200	200	50	7	200	200	200	200
8	200	200	200	50	8	200	200	200	200
9	200	200	200	200	9	200	200	200	50
10	500	500	100	200	10	200	200	200	200
11	500	500	50	50	11	500	500	100	500
12	500	500	500	50	12	50	50	50	50
13	1000	1000	1000	1000	13	50	50	50	50
14	1000	1000	1000	1000	14	1000	1000	1000	1000
					15	1000	1000	1000	1000

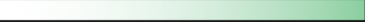
	Positive selection AP	Negative selection AP	
Very high stringency	AP _{T3} -VAMP7	AP _{neg} -VAMP1a	
High stringency	AP _{T3} -VAMP7	AP _{neg} -VAMP1b	10 ² pfu/mL  10 ⁹ pfu/mL
Moderate stringency	AP _{T3} -VAMP7	AP _{neg} -VAMP1c	
Low stringency	AP _{T3} -VAMP7	AP _{neg} -VAMP1d	

Figure S13. Phage passage schedule for F(3230) protease evolution in PANCE using the dual positive and negative selection. The numbers in each cell indicate the dilution factor for the input phage population, while the shading indicates the output titer on the scale at the bottom. Purple outlines indicate populations that were used to inoculate subsequent passages, identified with bolded purple text. Populations sequenced at the end of the PANCE campaign are indicated in orange text. Populations were only mixed within replicates, not between replicates.

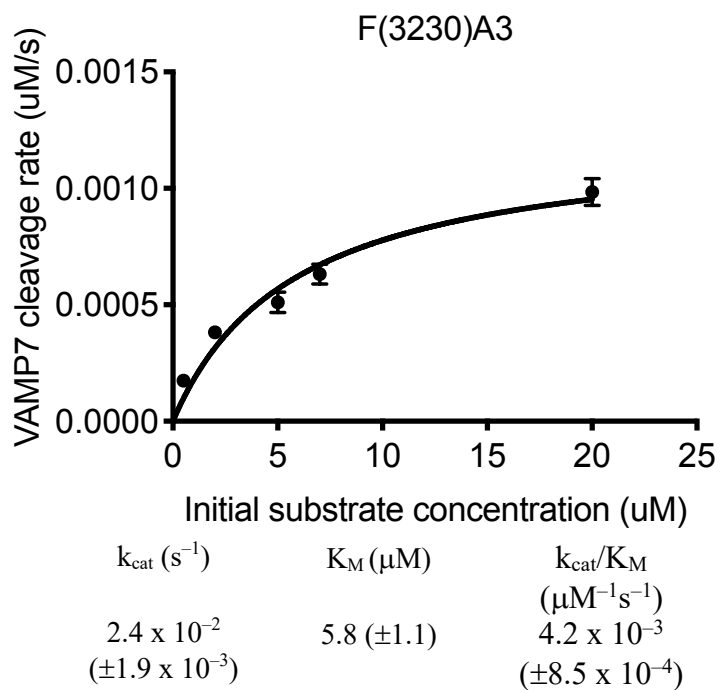


Figure S14. Kinetic analysis of the evolved F(3230)A3 protease. Values and error bars represent the mean and standard deviation of three independent replicates.

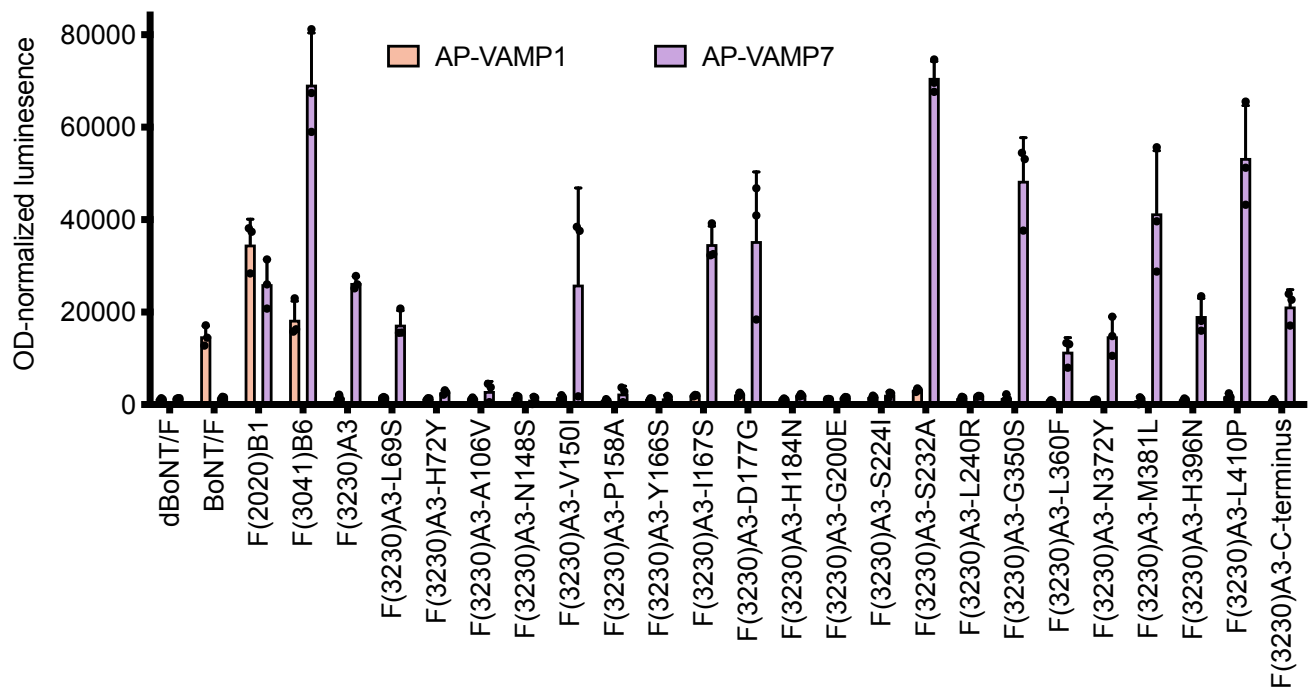


Figure S15. Luciferase activity assay of reversion mutants of F(3230)A3 protease on VAMP1 and VAMP7 substrates. dBoNT/F is an inactive BoNT/F protease mutant used as a negative control. Values and error bars represent the mean and standard deviation of three independent biological replicates.

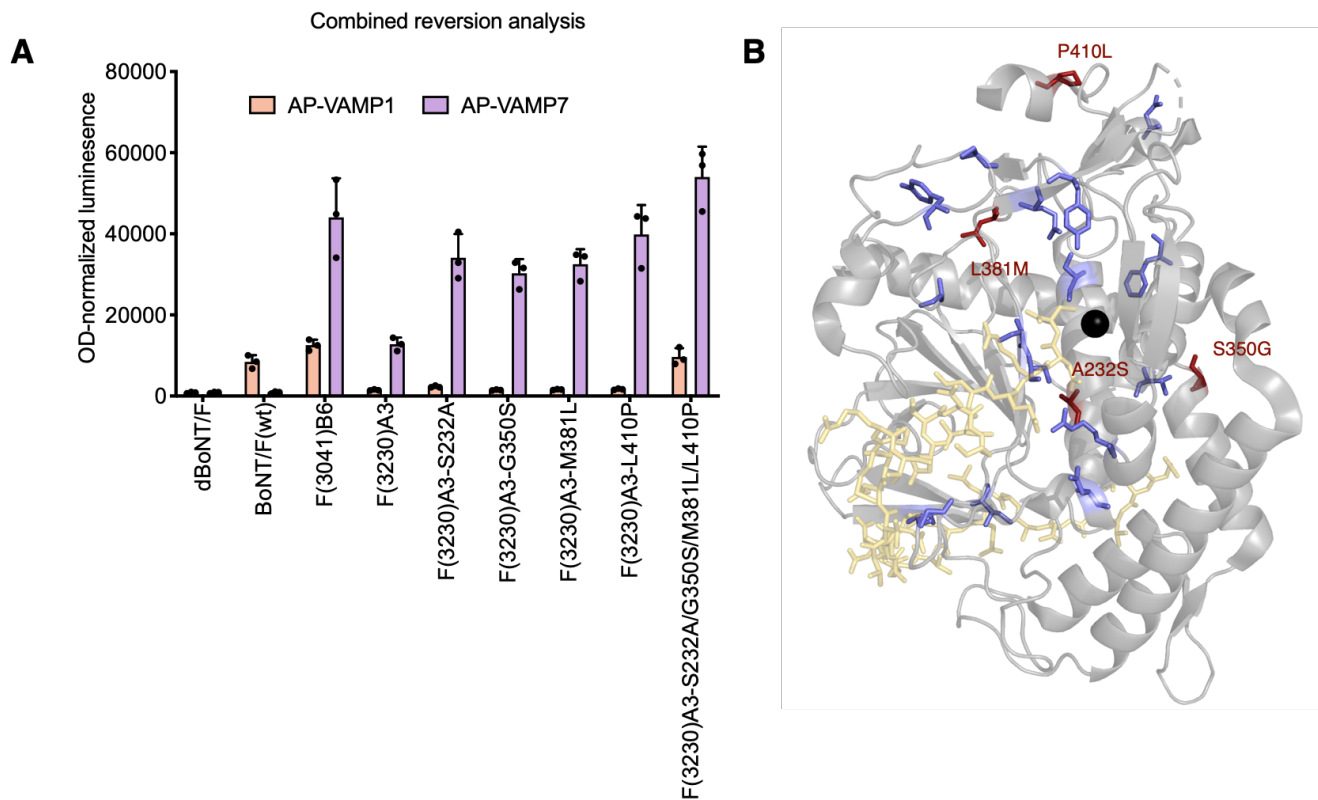
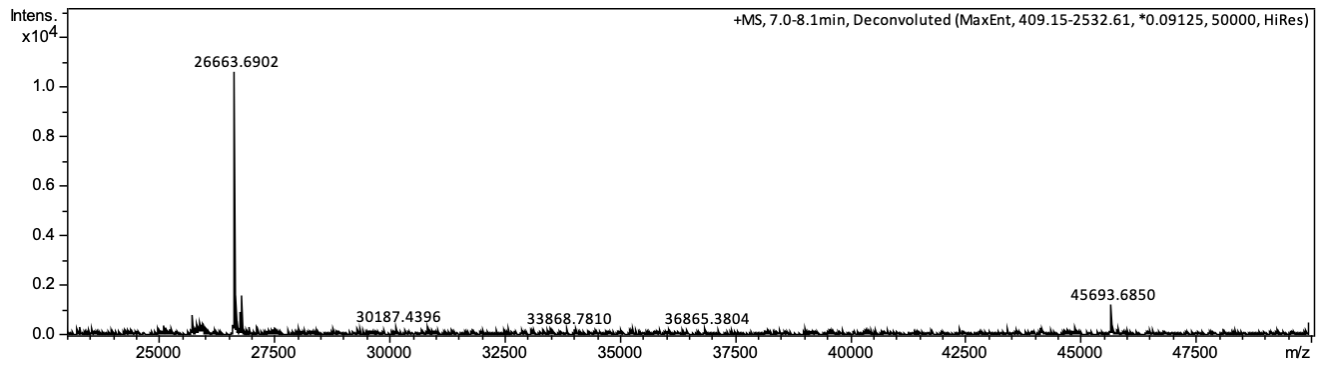


Figure S16. (A) Luciferase activity assay of reversion mutants of F(3230)A3 on VAMP1 and VAMP7 substrates. dBoNT/F is an inactive BoNT/F protease mutant used as a negative control. Values and error bars represent the mean and standard deviation of three independent biological replicates. (B) BoNT/F light chain crystal structure (PDB: 3FIE). VAMP2 substrate mimic is shown in yellow, the active site zinc atom is shown as a black sphere, and mutated residues present in F(3230)A3 are shown in blue or red. Residues targeted for reversion in (A) are highlighted in red.



MKIEEGKLVWINGDKGYNGLAEVGGKFEKDTGIKVTVEHPDKLEEKFPQVAATGDGPDIIIFWAHDRFGGY
 AQSGLLAEITPDKAFQDKLYPFTWDAVRYNGKLIAYPIAVEALSLIYNKDLLPNPPKTWEEIPALDKELKAKG
 KSALMFNLQEPYFTWPLIAADGGYAFKYENGYDIKDVGVNAGAKAGLTFVLVDLIKHKHMNADTDYSIAE
 AAFNKGETAMTINGPWAWNSNIDTSKVNYGVTVLPTFKGQPSKPFVGVLSAGINAASPNKELAKEFLENYL
 LTDEGLEAVNKDKPLGVAALKSYEEELAKDPRIAATMENAQKGEIMPNIQMSAFWYAVRTAVINAASGRQ
 TVDEALKDAQTNSSSGGS**KGLDKV****METQAQVDELK****GIMVRNIDLVAQRGERLELLIDKTE**

Expected (m/z): 45694.97
 Found (m/z): 45693.69

NLV**DSSVTFK****TTSRNLAR**GGSHPPYTITYFPVRGRCEAMRMLLADQDQSWKEEVVMTETWPLKPSCLF
 RQLPKFQDGDLTLYQSNAILRHLGRSFGLYGKDQKEAALVDMVNDGVEDLRCKYATLIYTNYEAGKEKYV
 KELPEHLKPFETLLSQNGGQAFVVGSIQSFADYNLLDLLRIHQVLPNSCLDAFPLLSAYVARLSARPKIKA
 FLASPEHVNRPINGNGKQHHHHHH

Expected (m/z): 26663.42
 Found (m/z): 26663.69

Figure S17. Identification of the cleavage site of VAMP7 by mF(3230)A3 protease. Assay was performed using 2 μ M MBP-VAMP7(K121–A181)-GST substrate, with 100 nM protease, then analyzed by LCMS for average intact mass. VAMP7(K121–R180) sequence is indicated in red.

		Relative cleavage rate
VAMP1	L E R D Q K L S E L D D R A D A L Q A G A	N.D
VAMP1(E64L)	L E R D Q K L S L L D D R A D A L Q A G A	0.02
VAMP1(D66I)	L E R D Q K L S E L I D R A D A L Q A G A	0.09
VAMP1(A69T)	L E R D Q K L S E L D D R T D A L Q A G A	N.D
VAMP1(A71N)	L E R D Q K L S E L D D R A D N L Q A G A	0.03
VAMP1(A64L/D66I/A69T/A71N)	L E R D Q K L S L L I D R T D N L Q A G A	1.56
VAMP7	A Q R G E R L E L L I D K T E N L V D S S	1

Figure S18. Substrate sequence-activity relationships for F(3230)A3 cleavage of VAMP7. Cleavage sites for wild-type BoNT/F protease and F(3230)A3 are indicated by orange and black wedges, respectively. The VAMP1 sequence shown covers L56–A76, while the VAMP7 sequence shown covers A148–S168. N.D. = not detected.

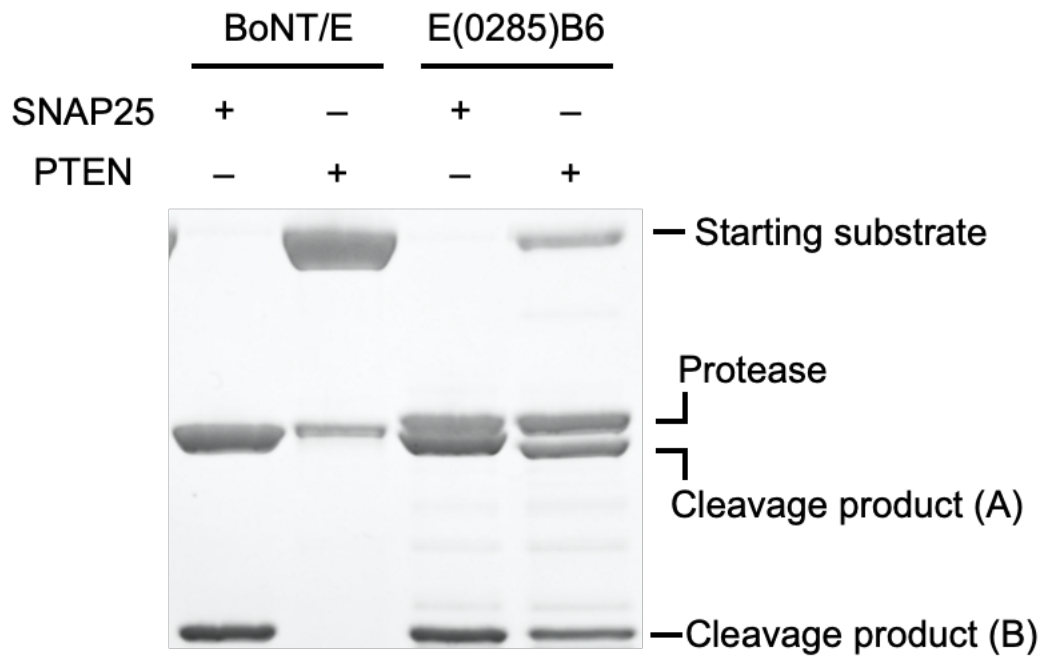


Figure S19. *In vitro* assessment of E(0285)B6 selectivity on SNAP-25(M167–D186) and PTEN(N292–N311) cleavage sequences. Substrates were assayed as peptide fragments in between an N-terminal MBP tag, and a C-terminal GST tag. Reactions were performed with 0.7 μ M protease and 5 μ M substrate.

Passage number	Replicate A input phage dilution factor				Replicate B input phage dilution factor				Replicate C input phage dilution factor			
	Low stringency	Moderate stringency	High stringency	Very high stringency	Low stringency	Moderate stringency	High stringency	Very high stringency	Low stringency	Moderate stringency	High stringency	Very high stringency
1	100	100	100	100	100	100	100	100	100	100	100	100
2	100	100	100	100	100	100	100	100	100	100	100	100
3	100	100	100	100	100	100	100	100	100	100	100	100
4	100	100	100	100	100	100	100	100	100	100	100	100
5	100	100	100	100	100	100	100	100	100	100	100	100
6	400	400	400	400	400	400	400	400	400	400	400	400
7	400	400	400	400	400	400	400	400	400	400	400	400
8	1000	1000	1000	1000	1000	1000	1000	1000	1000	1000	1000	1000
9	1000	1000	1000	1000	1000	1000	1000	1000	1000	1000	1000	1000
10	1000	1000	1000	1000	1000	1000	1000	1000	1000	1000	1000	1000
11	1000	1000	1000	1000	1000	1000	1000	1000	1000	1000	1000	1000
12	250	250	250	250	250	250	250	250	250	250	250	250
13	2000	2000	2000	2000	2000	2000	2000	2000	2000	2000	2000	2000
14	2000	2000	2000	2000	2000	2000	2000	2000	2000	2000	2000	2000
15	5000	5000	5000	5000	5000	5000	5000	5000	5000	5000	5000	5000


	Positive selection AP	Negative selection AP	
Very high stringency	AP _{T3} -PTEN	AP _{neg} -SNAP25a	
High stringency	AP _{T3} -PTEN	AP _{neg} -SNAP25b	10 ² pfu/mL  10 ⁹ pfu/mL
Moderate stringency	AP _{T3} -PTEN	AP _{neg} -SNAP25c	
Low stringency	AP _{T3} -PTEN	AP _{neg} -SNAP25d	

Figure S20. Phage passage schedule for E(4130) protease evolution in PANCE using the dual positive and negative selection. The numbers in each cell indicate the dilution factor for the input phage population, while the shading indicates the output titer on the scale at the bottom. Blue outlines indicate populations that were used to inoculate subsequent passages, identified with blue text. Populations sequenced at the termination of the PANCE campaign are indicated in orange text. Populations were only mixed within replicates, not between replicates.

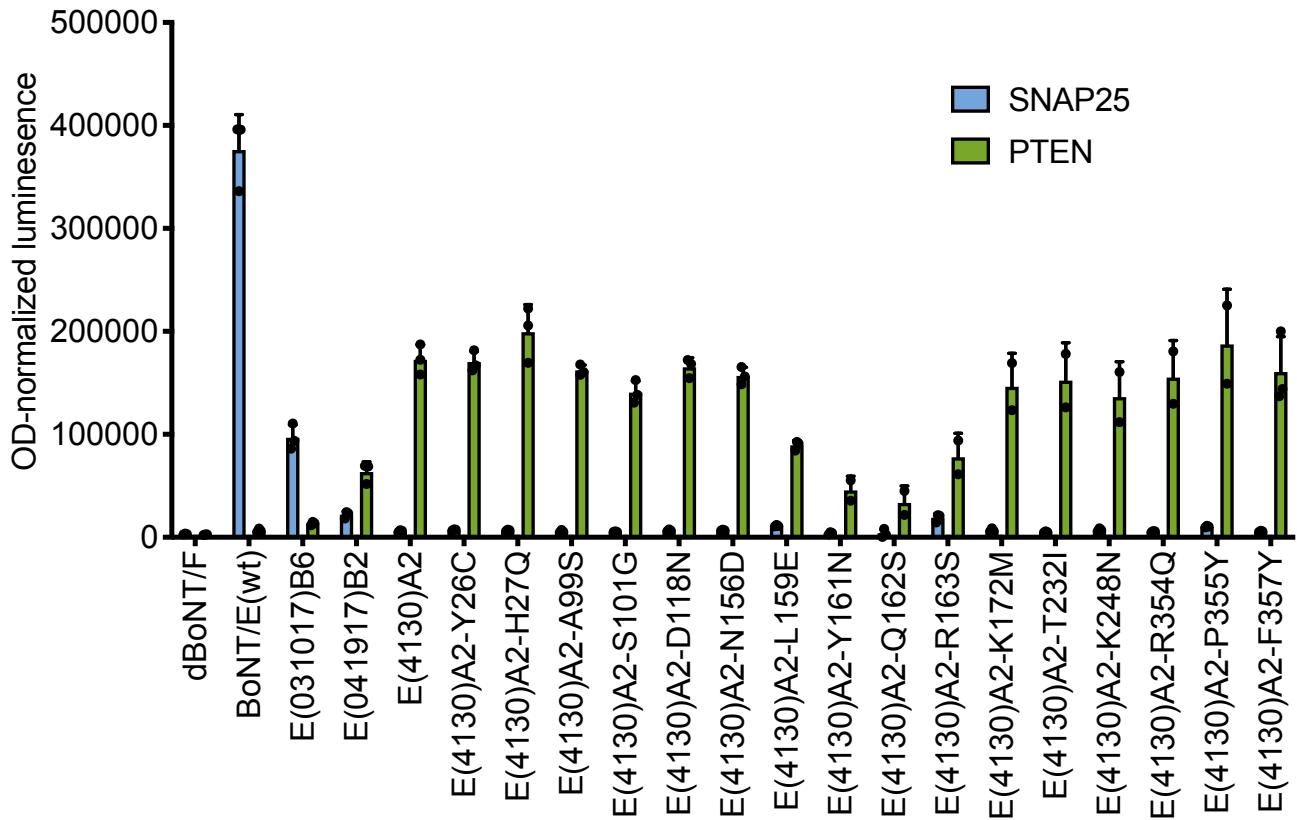
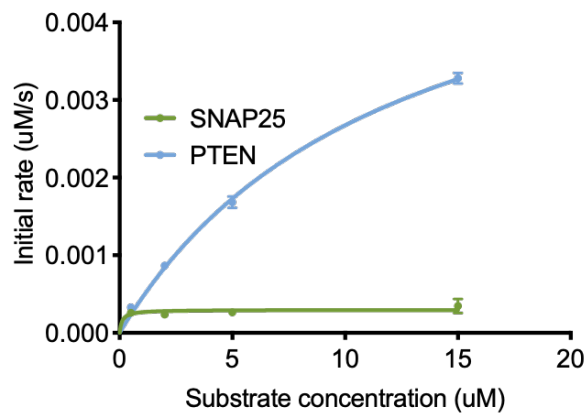
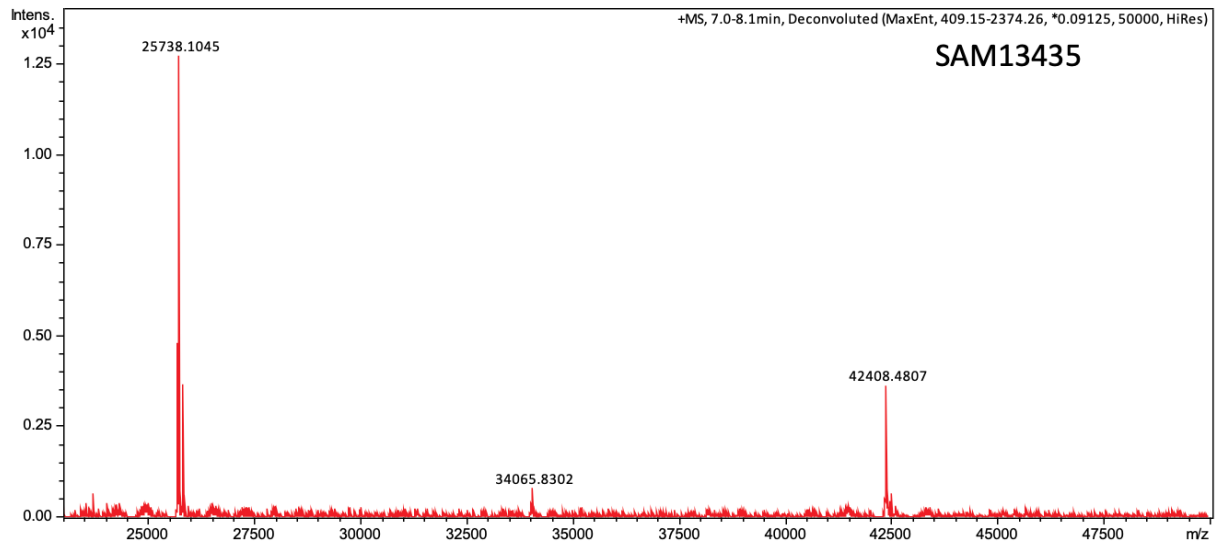


Figure S21. Luciferase activity assay of reversion mutants of E(4130)A2 on SNAP25 and PTEN substrates. Values and error bars represent the mean and standard deviation of 2–3 independent biological replicates.



Substrate	k_{cat} (s^{-1})	K_M (μM)	k_{cat}/K_M
PTEN	0.59	12.04	4.9×10^{-2}
SNAP25	2.9×10^{-2}	0.113	0.263

Figure S22. Michaelis-Menten kinetic analysis of E(4130)A2 on SNAP-25 and PTEN. Reactions were performed using indicated concentrations of substrates and 10 nM protease.



MKIEEGKLVIIWINGDKGYNGLAEVGKKFEKDTGIKVTVEHPDKLEEKFPQVAATGDGPDIIIFWAHDFGGY
 AQSGLLAEITPDKAFQDKLYPFTWDAVRYNGKLIAYPIAVEALSIIYNKDLLPNPPKTWEEIPALDKELKAKG
 KSALMFNLQEPYFTWPLIAADGGYAFKYENGYDIKDVGVNDAGAKAGLTLFLVDLIKHKHMNADTDYSIAE
 AAFNKGETAMTINGPWAWSNIDTSKVNYGVTVLPFKGQPSKPFVGVLSAGINAASPNKELAKEFLENYL
 LTDEGLEAVNKDKPLGAVALKSYEEELAKDPRIAATMENAQKGEIMPNIQMSAFWYAVRTAVINAASGRQ
 TVDEALKDAQTNSSSGGGSGSE**NGSLCDQEIDS**

Expected (m/z): 42408.90
 Found (m/z): 42408.48

ICSIERADNGGSGGSPPYTITYFPVGRCEAMRMLLADQDQSWKEEVVMTETWPPLKPSCLFRQLPKFQ
 DGDLTLYQSNAILRHLGRSFLYGGKQKEAALVDMVNDGVEDLRCKYATLIYTNYEAGKEKYVKELPEHL
 KPFETLLSQNGGQAFVVGSIQSFADYNLLDLLRIHQVQLNPSCDAFPLLSAYVARLSARPKIKAFKFLASPEH
 VNRPINGNGKQHHHHHH

Expected (m/z): 25738.34
 Found (m/z): 25738.10

Figure S23. Identification of the cleavage site of PTEN by E(4130)A2. Assay was performed using 2 μ M MBP-PTEN(N292–N311)-GST substrate, with 100 nM protease, then analyzed by LCMS for average intact mass. PTEN(N292–N311) is indicated in red.

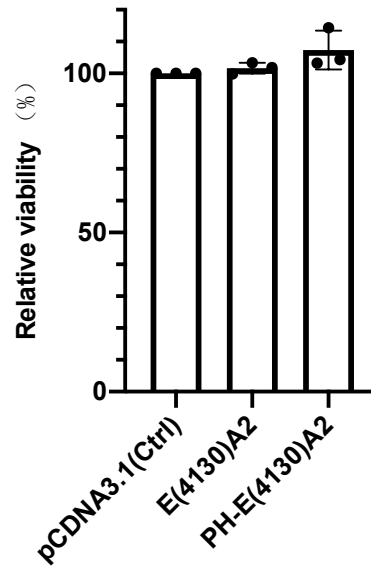


Figure S24. The viability of HEK293T cells 24 hours after transfection of E(4130)A2, PH-E(4130)A2, or empty pCDNA3.1 vector. All cell viabilities were normalized to cells transfected with pCDNA3.1 empty vector. No statistically significant differences were observed among all the groups analyzed by ordinary one-way ANOVA. Values and error bars represent the mean and standard deviation of three biological replicates.

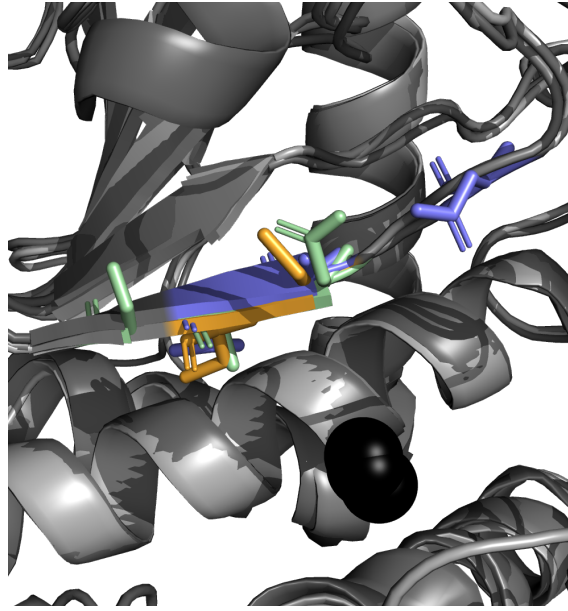


Figure S25. Structural alignment of the protease active site for BoNT/E (PDB 3D3X), BoNT/F (PDB 3FIE), and BoNT/X (PDB 6F47). The active site zinc metallocofactor is in black, and positions that evolved mutations are in green for BoNT/E (E159L, N161Y, S162Q, S163R), orange for BoNT/F (S166Y, S167I), and blue for BoNT/X (N164S, A166E, T167I).

Table S1. X(4130) protease genotypes observed after the final PANCE passages at high selection stringency from three replicates, with positive selection for Ykt6 cleavage and negative selection against VAMP1 cleavage. Mutations in orange were not present prior to the final 15 passages.

Position	23	98	100	113	133	143	144	148	166	167	175	169	218	225	241	257	267	268	279	285	314	322	341	345	349	364	391	413	416	425	434
Wild Type	R	V	E	E	D	N	N	N	A	T	I	G	A	L	N	R	L	L	S	K	Y	Q	T	V	S	L	S	S	L	R	YRNSKN
A.2	R	V	E	E	D	N	L	N	E	I	I	G	A	L	N	R	L	L	S	K	S	Q	T	V	S	L	S	S	L	R	YLNSKN
A.3	R	V	E	E	D	N	N	N	E	I	I	G	A	L	N	C	L	L	S	K	Y	K	T	V	S	I	S	F	L	R	YRNSKN
A.4	R	V	E	E	D	N	N	N	E	I	I	G	A	L	N	C	L	L	S	K	Y	K	T	V	S	L	S	S	L	R	YRNSKN
A.6	R	V	E	E	D	N	N	N	E	I	I	G	V	L	N	C	L	L	S	K	Y	K	T	V	S	I	S	F	L	R	YRNSKN
B.1	R	V	E	E	D	D	N	T	E	I	I	G	A	L	N	R	L	L	S	K	N	Q	T	V	S	I	S	S	L	R	YRNSKN
B.2	R	V	E	E	D	N	N	N	E	I	I	G	A	L	N	R	L	L	S	K	Y	K	T	V	S	V	S	S	L	R	YLNSKN
B.3	R	V	E	E	D	D	N	T	E	I	I	G	A	L	N	R	L	L	S	K	C	Q	T	V	S	I	S	S	L	R	YRNSKN
B.4	R	G	E	K	D	D	N	T	E	I	I	G	A	L	N	R	L	L	S	K	Y	Q	T	E	S	I	S	S	L	R	YRNSKN
B.5	S	G	E	E	D	N	N	N	E	I	I	G	A	L	N	R	L	L	S	K	Y	Q	T	V	S	L	S	S	L	R	YRNSKN
B.6	R	V	E	E	N	N	N	S	E	I	I	G	A	L	N	R	L	L	P	K	Y	Q	T	V	S	L	S	S	L	R	YLNSKN
B.7	R	V	E	E	D	N	N	N	E	I	V	G	A	L	N	R	L	L	S	K	Y	Q	T	V	S	I	G	S	L	R	YRNSKN
B.8	R	G	D	E	D	D	N	T	E	I	I	G	A	L	N	R	L	L	P	K	Y	Q	T	V	S	L	S	S	F	R	YLNSKN
C.1	R	V	E	E	D	N	N	N	E	T	I	G	A	L	N	R	L	L	S	K	Y	Q	T	V	S	L	S	S	L	R	YRNSKN
C.2	R	V	E	E	D	D	N	N	E	T	I	G	A	L	N	C	I	I	S	K	Y	K	T	V	F	I	S	S	L	R	AFTATQKSNNGDFQHGLAQP*
C.3	R	V	E	E	D	D	N	N	E	T	I	G	A	L	N	R	L	L	S	K	Y	Q	T	V	S	L	S	S	L	R	YRNSKN
C.4	R	V	E	E	D	D	N	N	E	T	I	G	A	W	N	C	I	I	S	K	Y	Q	P	V	F	I	S	S	L	R	AFTATQKSNNGDFQHGLAQP*
C.5	R	V	E	E	D	N	N	N	E	I	I	G	V	L	N	R	L	L	S	K	Y	Q	T	V	S	L	S	S	L	R	YRNSKN
C.6	R	V	E	E	D	N	N	T	E	A	I	G	V	L	I	R	L	L	S	N	Y	Q	T	V	S	L	S	S	L	R	YRNSKN
C.7	R	V	E	E	D	D	N	N	E	T	I	R	A	L	N	R	L	L	S	K	Y	Q	T	V	S	L	S	S	L	R	YRNSKN
C.8	R	V	E	E	D	D	N	N	E	T	I	G	A	L	N	C	I	I	S	K	Y	Q	T	V	F	I	S	S	L	R	AFTATQKSNNGDFQHGLAQP*

Table S2. X-ray crystallography data collection and refinement statistics for structural characterization of evolved BoNT/X(4130)B1 protease.

Crystallography Data	
Wavelength (Å)	0.97856
Space group	P2 ₁ 2 ₁ 2 ₁
Unit Cell	
<i>a</i> , <i>b</i> , <i>c</i> (Å)	59.94, 86.78, 93.56
α , β , γ (°)	90.00, 90.00, 90.00
Resolution (Å)	30.00 - 1.80 (1.83-1.80) ^a
No. of reflections	46,066 (2,287)
R _{sym} (%) ^b	6.1 (77.9)
I/ σ (I)	31.0 (2.6)
Completeness (%)	100.0 (100.0)
Redundancy	7.2 (7.1)
Wilson <i>B</i> factor (Å ²)	25.7
Refinement (F>0)	
Resolution (Å)	29.97 - 1.80 (1.85 - 1.80)
No. of reflections	45,938 (3,354)
Completeness (%)	100.0 (100.0)
R _{work} /R _{free} (%) ^c	15.1/18.5 (23.6/24.6)
No. of non-H atoms	
Protein	3,468
Zn ²⁺	1
Ligands (EDO, GOL)	40
Water	407
Average B-factors (Å ²)	
Protein	29.7
Zn ²⁺	25.5
Ligand	50.1
Water	37.5
Coordinate Deviations	
RMSD bonds (Å)	0.006
RMSD angle (°)	1.353
Ramachandran plot	
Favored (%)	96
Allowed (%)	4
Outside allowed (%)	0

^aNumbers in parentheses refer to the highest resolution shells

^b $R_{\text{sym}} = \sum_h \sum_i |I_i(h) - \langle I(h) \rangle| / \sum_h \sum_i I_i(h)$, where $I_i(h)$ is the i th measurement of reflection h , and $\langle I(h) \rangle$ is the weighted mean of all measurement of h .

^c $R = \sum_h ||F_{\text{obs}}| - |F_{\text{cal}}|| / \sum_h |F_{\text{obs}}|$, where F_{obs} and F_{cal} are the observed and calculated structure factor, respectively. R_{work} and R_{free} were calculated by using the working and test set reflections, respectively.

Table S3. X(5010) protease genotypes after the final PANCE passages at high selection stringency from three replicates, with positive selection for VAMP4 cleavage and negative selection against VAMP1 cleavage. Mutations in orange were not present prior to the final 12 passages.

Position	3	26	65	71	128	143	150	164	166	168	174	222	223	224	240	257	294	313	314	322	339	364	366	410	423	C-TERM
Wild type	L	R	I	M	A	N	Q	N	A	Y	P	A	S	T	S	R	Y	K	Y	Q	L	L	E	K	C	LLYNAIYRNSKN
A.1	L	R	I	M	A	D	Q	S	A	C	P	A	S	I	K	R	C	K	H	Q	L	L	E	K	Y	LLYNAIYRNSKN
A.2	I	R	I	M	A	D	Q	S	A	C	P	A	S	I	K	R	C	K	Y	Q	L	L	E	N	C	LLYNAIYRNSKN
A.3	L	R	V	M	A	D	Q	S	A	C	P	A	L	I	K	R	C	K	Y	Q	L	L	E	K	C	LLYNAIYRNSKN
A.4	L	FS	I	M	A	D	Q	S	A	C	P	A	S	I	K	R	C	K	H	Q	L	L	E	K	C	LLYNAIYRNSKN
A.5	L	R	I	M	V	D	Q	S	A	C	P	A	S	I	K	R	C	K	H	Q	L	L	E	K	C	LLYNAIYRNSKN
A.7	L	R	I	M	A	D	Q	S	A	C	P	A	S	I	K	R	C	K	H	Q	L	F	E	K	C	LLYNAIYRNSKN
B.1	L	R	I	M	A	D	Q	S	E	Y	T	S	S	I	K	R	Y	R	Y	Q	L	L	E	K	C	LLYNAIYRNSKN
B.2	L	R	I	M	A	D	Q	S	E	Y	T	S	S	I	K	R	Y	R	Y	Q	L	L	E	K	C	LLYNAIYRNSKN
B.3	L	R	I	M	A	D	Q	S	E	Y	T	S	S	I	K	R	Y	R	Y	Q	L	L	D	K	C	LLYNAIYRNSKN
B.4	L	R	I	V	A	D	Q	S	E	Y	T	S	S	I	K	R	Y	R	Y	Q	L	L	E	K	C	LLYNAIYRNSKN
B.5	L	R	I	M	A	D	Q	S	E	Y	T	S	S	I	K	R	Y	R	Y	Q	L	L	E	K	C	LLYNAIYRNSKN
B.6	L	R	I	M	A	D	Q	S	E	Y	T	S	S	I	K	R	Y	R	Y	Q	L	L	E	K	C	LLYNAIYRNSKN
B.7	L	R	I	M	A	D	Q	S	E	Y	T	S	S	I	K	R	Y	R	Y	Q	L	L	E	K	C	LLYNAIYRNSKN
C.1	L	R	I	M	A	N	K	D	A	Y	P	A	S	I	K	R	Y	N	Y	E	F	L	E	K	C	LLYNAIYRNSKN
C.2	L	R	I	M	A	D	Q	S	E	Y	T	S	S	I	K	R	Y	R	Y	Q	L	L	E	K	C	LLYNAIYRNSKN
C.3	L	R	I	M	A	N	Q	E	A	Y	P	A	S	I	K	R	Y	N	Y	E	F	L	E	K	C	LLYNAIYRNSKN
C.6	L	R	I	M	A	N	Q	D	A	Y	P	A	S	I	K	C	Y	N	Y	E	F	F	E	K	C	CCIMPFTATQKTNNGDFQHGLAQP
C.7	L	R	I	M	A	N	Q	D	A	Y	P	A	S	I	K	C	Y	N	Y	E	F	F	E	K	C	LLYNAIYRNSKN
C.8	L	R	I	M	A	N	Q	D	A	Y	P	A	S	I	K	C	Y	N	Y	E	F	F	E	K	C	CCIMPFTATQKTNNGDFQHGLAQP

Table S4. PACE selection schedule for the evolution of a VAMP7-cleaving BoNT/F protease variant.

<u>PACE-F(0067)</u>				
Input phage	Phase 1 APs	Phase 2 AP	Phase 3 APs	Output phage
SP-BoNT/F	AP-VAMP1	AP-VAMP1	AP-VAMP1	SP-F(0067)
<u>PACE-F(1006)</u>				
Input phage	Phase 1 APs	Phase 2 APs	Phase 3 APs	Output phage
SP-F(0067)	AP-VAMP1	AP-VAMP1 + AP-SS.F1	AP-SS.F1	SP-F(1006A)
<u>PACE-F(1023)</u>				
Input phage	Phase 1 APs	Phase 2 APs	Phase 3 APs	Output phage
SP-F(1006A)	AP-SS.F1	AP-SS.F1 + AP-SS.F2	AP-SS.F2	SP-F(1023A)
<u>PACE-F(1037)</u>				
Input phage	Phase 1 APs	Phase 2 APs	Phase 3 APs	Output phage
SP-F(1023A)	AP-SS.F1	AP-SS.F1 + AP-SS.F2	AP-SS.F2	SP-F(1037A)
SP-F(1023A)	AP-SS.F2	AP-SS.F2	AP-SS.F2	SP-F(1037B)
SP-F(1023A)	AP-SS.F2	AP-SS.F2	AP-SS.F2	SP-F(1037C)
<u>PACE-F(1131)</u>				
Input phage	Phase 1 APs	Phase 2 APs	Phase 3 APs	Output phage
SP-F(1037A)	AP-SS.F2	AP-SS.F2 + AP-SS.F3	AP-SS.F3	SP-F(1131A)
SP-F(1037B)	AP-SS.F2	AP-SS.F2 + AP-SS.F3	AP-SS.F3	SP-F(1131B)
SP-F(1037C)	AP-SS.F2	AP-SS.F2 + AP-SS.F3	AP-SS.F3	SP-F(1131C)
<u>PACE-F(1216)</u>				
Input phage	Phase 1 APs	Phase 2 APs	Phase 3 APs	Output phage
SP-F(1131A)	AP-SS.F3	AP-SS.F3 + AP-SS.F4	AP-SS.F4	SP-F(1216A)
SP-F(1131B)	AP-SS.F3	AP-SS.F3 + AP-SS.F4	AP-SS.F4	SP-F(1216B)
SP-F(1131C)	AP-SS.F3	AP-SS.F3 + AP-SS.F4	AP-SS.F4	SP-F(1216C)
<u>PACE-F(2016)</u>				
Input phage	Phase 1 APs	Phase 2 APs	Phase 3 APs	Output phage
SP-F(1216A)	AP-SS.F4	AP-SS.F4 + AP-SS.F7	AP-SS.F7	SP-F(2016A)
SP-F(1216B)	AP-SS.F4	AP-SS.F4 + AP-SS.F7	AP-SS.F7	SP-F(2016B)
SP-F(1216C)	AP-SS.F4	AP-SS.F4 + AP-SS.F7	AP-SS.F7	SP-F(2016C)
<u>PACE-F(2020)</u>				
Input phage	Phase 1 APs	Phase 2 APs	Phase 3 APs	Output phage
SP-F(2016A)	AP-SS.F7	AP-SS.F7 + AP-VAMP7(low)	AP-VAMP7(low)	SP-F(2020A)
SP-F(2016B)	AP-SS.F7	AP-SS.F7 + AP-VAMP7(low)	AP-VAMP7(low)	SP-F(2020B)
SP-F(2016C)	AP-SS.F7	AP-SS.F7 + AP-VAMP7(low)	AP-VAMP7(low)	SP-F(2020C)
<u>PACE-F(3041)</u>				
Input phage	Phase 1 APs	Phase 2 APs	Phase 3 APs	Output phage
SP-F(2020)A.B.C	AP-VAMP7(low)	AP-VAMP7(low) + AP-VAMP7(high)	AP-VAMP7(high)	SP-F(3041A)
SP-F(2020)A.B.C	AP-VAMP7(low)	AP-VAMP7(low) + AP-VAMP7(high)	AP-VAMP7(high)	SP-F(3041B)

Table S5. Representative F(3041) protease genotypes observed from two PACE replicates. The evolution used positive selection for VAMP7 cleavage and negative selection against VAMP1 cleavage. Mutations in purple were not enriched prior to high-stringency PACE selection.

Position	29	31	72	99	101	106	113	131	141	150	155	166	167	174	177	178	184	193	200	210	214	215	224	240	267	270	293	297	303	335	350	360	372	396	410	418	420	423		
Wild type	K	K	Y	N	N	V	C	V	V	Y	V	T	V	M	G	G	N	V	E	Y	T	E	S	R	F	F	N	I	R	T	S	F	Y	N	P	D	G	E		
A	2		H			A			T		Y	I				T		G	H			I	L							G	L	H	H	L		420(AWLRKS*)				
	3		H			A			T		Y	I						G				I	L							G	L	H	H	L		420(AWLRKS*)				
	4		H			A			T		Y	I					T		G			G	I	L						G	L	H	H	L		420(AWLRKS*)				
	5		N	H	S		A				Y	I					A		G			I	L							G	L	H	H	L		420(AWLRKS*)				
	6						A				Y	I							M				G							G	L	H	H	L		420(AWLRKS*)				
	7						A				Y	I						K		G				I	F				L		S			L	H	H	L	Y	F420S	K
	8			S			A				Y	I							G				G	I	L	I	V						L	H	H	L	Y		K	
	B	2					A				Y	I						M		G			I	L						G	L	H	H	L		420(AWLRKS*)				
4		E				A				T		Y	I	T				G				I	L							G	L	H	H	L		420(AWLRKS*)				
5				S	D		A			T		Y	I	T	A				G				I	L		V	D			C			G	L	H	H	L		420(AWLRKS*)	
6				H			A		G	T		Y	I	T					G				I	L						G	L	H	H	L		420(AWLRKS*)				
7							A				I	Y	I	T						G				I	L					G	L	H	H	L		420(AWLRKS*)				
8				H			A		G		Y	I						M		G			I	L					G	L	H	H	L		420(AWLRKS*)					

Table S6. Representative F(3230) genotypes observed after the final PANCE passages from one of two replicates, with positive selection for VAMP7 cleavage and negative selection against VAMP1 cleavage. Mutations in purple emerged during negative selection.

	Position	4	8	45	51	60	69	72	99	105	106	113	131	134	137	148	150	158	166	167	174	177	183	184	199	200	204	210	224	232	233	240	253	264	270	277	292	297	325	350	358	360	369	372	376	381	396	400	410	420		
	Wild Type	V	F	I	T	D	S	Y	N	E	V	Y	V	T	V	S	I	A	S	S	M	G	S	N	Y	E	N	Y	S	A	L	R	A	L	F	I	I	I	G	S	N	F	F	Y	K	L	N	N	P	GLVEKIVK		
Very high stringency	a	V	F	I	T	V	S	H	S	D	A	Y	F	T	V	S	I	A	Y	I	M	G	S	N	Y	G	N	C	I	A	L	L	A	L	V	I	T	M	G	G	N	L	Y	H	K	L	H	N	P	AWLRKIS		
	b	V	F	I	T	V	S	H	S	D	A	Y	F	T	V	S	I	A	Y	I	M	G	S	N	Y	G	N	C	I	A	L	L	A	L	V	I	T	M	G	G	N	L	Y	H	K	L	H	N	P	AWLRKIS		
	c	V	F	I	T	D	L	H	N	E	A	Y	V	T	V	N	V	P	Y	I	M	D	S	H	Y	G	N	Y	I	S	L	L	A	L	F	I	I	I	G	G	N	L	F	N	K	L	H	N	L	AWLRKIS		
	d	V	F	I	T	D	S	H	S	D	A	Y	F	T	V	S	I	A	Y	I	M	G	S	N	Y	G	N	C	I	A	L	L	A	L	V	I	I	M	G	G	N	L	F	H	K	L	H	N	P	AWLRKIS		
	e	V	L	I	T	D	S	H	S	D	A	Y	F	T	V	S	I	A	Y	I	M	G	S	N	Y	G	N	C	I	A	L	L	A	L	V	I	I	M	G	G	N	L	Y	H	E	L	H	N	P	AWLRKIS		
	f	V	F	I	T	D	S	H	S	D	A	Y	F	T	V	S	I	A	Y	I	M	G	S	N	Y	G	N	C	I	A	L	L	A	L	V	I	I	M	G	G	N	L	F	N	K	L	H	N	P	AWLRKIS		
	g	V	F	I	T	D	L	H	N	E	A	Y	V	A	V	N	I	P	Y	I	M	D	S	H	Y	G	N	Y	I	S	L	L	A	L	F	I	I	I	G	G	N	L	F	N	K	L	H	N	L	AWLRKIS		
	h	V	L	I	T	D	S	H	S	D	A	Y	F	T	V	S	I	A	Y	I	M	G	S	N	Y	G	N	C	I	A	L	L	A	L	V	I	I	M	G	G	N	L	Y	H	E	L	H	N	P	AWLRKIS		
High stringency	a	V	F	I	T	D	L	H	N	E	A	Y	V	T	V	N	I	P	Y	I	M	G	S	N	Y	G	N	Y	I	S	L	L	A	L	V	I	I	I	G	G	N	L	F	N	K	L	H	S	L	AWLRKIS		
	b	V	F	I	T	D	L	H	N	E	A	Y	V	T	V	N	I	P	Y	I	M	G	S	N	Y	G	N	Y	I	S	L	L	A	L	V	I	I	I	G	G	N	L	F	N	K	L	H	N	L	AWLRKIS		
	c	V	F	I	T	D	L	H	N	E	A	Y	V	T	V	N	I	P	Y	I	M	G	S	H	Y	G	N	Y	I	S	F	L	A	L	V	I	I	I	G	G	N	L	F	N	K	L	H	N	L	AWLRKIS		
	d	V	L	I	T	D	S	H	S	D	A	Y	F	T	V	S	I	A	Y	I	M	G	S	N	Y	G	N	C	I	A	L	L	A	L	V	I	I	M	G	G	N	L	Y	H	E	L	H	N	P	AWLRKIS		
	e	V	L	I	T	D	S	H	S	D	A	Y	F	T	V	S	I	A	Y	I	M	G	S	N	Y	G	N	C	I	A	L	L	A	L	V	I	I	M	G	G	N	L	Y	H	E	L	H	N	P	AWLRKIS		
	f	V	L	I	T	D	S	H	S	D	A	Y	F	T	V	S	I	A	Y	I	M	G	S	N	Y	G	N	C	I	A	L	L	A	L	V	I	I	M	G	G	N	L	Y	H	E	L	H	N	P	AWLRKIS		
	g	V	F	I	T	D	S	H	S	D	A	Y	F	T	V	S	I	A	Y	I	M	G	S	N	Y	G	N	C	I	A	L	L	A	L	V	V	I	M	G	G	N	L	F	P	K	L	H	N	P	AWLRKIS		
	h	V	F	I	T	D	L	H	N	E	A	Y	V	T	V	N	I	P	Y	L	M	G	S	H	Y	G	N	Y	I	S	L	L	A	L	F	I	I	I	G	G	S	L	F	N	K	L	H	N	L	AWLRKIS		
Moderate stringency	a	V	F	I	T	D	L	H	N	E	A	Y	V	T	V	N	I	P	Y	I	V	G	S	H	Y	G	N	Y	I	S	L	L	A	L	F	I	I	I	G	G	N	L	F	N	K	L	H	N	L	AWLRKIS		
	b	V	F	I	T	D	L	H	N	E	A	Y	V	T	V	S	I	P	Y	I	V	G	S	H	Y	G	N	Y	I	S	L	L	A	L	F	I	I	I	G	G	N	L	F	N	K	L	H	N	L	AWLRKIS		
	c	V	F	I	T	D	L	H	N	E	A	Y	F	T	V	N	I	P	Y	L	M	G	S	N	Y	G	N	Y	I	S	L	L	A	L	F	I	I	I	G	G	N	L	F	N	K	L	H	N	L	AWLRKIS		
	d	V	F	I	T	D	L	H	N	E	A	Y	V	T	I	N	I	P	Y	I	V	G	S	H	Y	G	N	Y	I	S	L	L	A	L	T	L	F	I	I	I	G	G	N	L	F	N	K	L	H	N	L	AWLRKIS
	e	V	F	I	T	D	L	H	N	E	A	Y	V	T	V	N	I	P	Y	I	M	G	S	H	Y	G	N	Y	I	S	L	L	A	L	F	I	I	I	G	G	N	L	F	N	K	L	H	N	L	AWLRKIS		
	f	V	F	I	T	D	S	H	S	E	A	Y	V	T	V	S	I	A	Y	L	M	G	S	N	Y	G	S	C	I	A	L	L	A	L	V	I	I	I	G	G	N	L	F	H	K	L	H	N	P	AWLRKIS		
	g	V	F	I	T	D	L	H	N	E	A	Y	V	T	V	N	I	P	Y	I	M	D	S	H	Y	G	N	Y	I	S	L	L	A	L	F	I	I	I	G	G	N	L	F	N	K	L	H	N	L	AWLRKIS		
	h	V	F	I	T	D	S	H	N	E	A	Y	V	T	V	S	I	P	Y	I	T	G	S	H	Y	G	N	Y	I	S	L	L	A	L	F	I	I	I	G	G	N	L	F	N	K	L	H	N	L	AWLRKIS		
Low stringency	a	V	F	I	T	D	S	H	S	D	A	Y	F	T	V	S	I	A	Y	I	M	G	S	N	Y	G	N	C	I	A	L	L	A	L	V	I	I	M	D	G	N	L	F	H	K	L	H	N	P	AWLRKIS		
	b	V	F	I	T	D	L	H	N	E	A	Y	F	T	V	N	I	P	Y	I	M	G	S	N	Y	G	N	Y	I	S	L	L	A	L	F	I	I	I	G	G	N	L	F	N	K	L	H	N	L	AWLRKIS		
	c	V	F	I	T	D	L	H	N	E	A	C	V	T	V	N	I	P	Y	I	M	G	N	H	Y	G	N	Y	I	S	L	L	A	L	F	I	I	I	G	G	N	L	F	N	K	L	H	N	L	AWLRKIS		
	d	V	F	I	T	D	L	H	N	E	A	C	V	T	V	N	I	P	Y	I	M	G	S	H	Y	G	N	Y	I	S	L	L	A	L	F	I	I	I	G	G	N	L	F	N	K	L	H	N	L	AWLRKIS		
	e	A	F	I	T	D	S	H	S	D	A	Y	F	T	V	S	I	A	Y	I	M	G	S	N	Y	G	N	C	I	A	L	L	A	L	V	I	I	M	G	G	N	L	F	H	K	L	H	N	P	AWLRKIS		
	f	V	F	I	T	D	L	H	N	E	A	C	V	T	V	N	I	P	Y	I	M	G	S	H	Y	G	N	Y	I	S	L	L	A	L	F	I	I	I	G	G	N	L	F	N	K	L	H	N	L	AWLRKIS		
	g	V	F	I	T	D	S	H	S	D	A	Y	F	T	V	S	I	A	Y	I	M	G	S	N	Y	G	N	C	I	A	L	L	A	L	V	I	I	M	G	G	N	L	F	H	K	L	H	N	P	AWLRKIS		
	h	V	F	I	T	D	S	H	N	E	A	Y	V	T	V	S	I	A	Y	I	M	G	S	N	Y	G	N	C	I	A	L	L	A	L	V	I	I	M	G	G	N	L	F	H	K	L	H	N	P	AWLRKIS		

Table S7. Relative cleavage efficiency of F(3041)B6 and F(3230)A3 proteases on VAMP family SNARE substrates, normalized to the VAMP7 cleavage rate. Reactions were performed using 50 nM protease with 5 mM substrate in 50 mM HEPES pH 7.3, 5 mM NaCl, 0.1% Tween-80, 2 mM DTT, 10 μ M Zn(OAc)₂. N.D. = not detected.

<u>Target</u>	<u>F(3041)B6</u>	<u>F(3230)A3</u>
VAMP1	0.05	0.02
VAMP2	0.05	0.04
VAMP3	0.06	0.03
VAMP4	0.05	N.D.
VAMP5	0.05	0.02
VAMP7	1	1
VAMP8	N.D.	N.D.
Ykt6	0.04	N.D.
Sec22b	0.15	0.05

Table S8. PACE selection schedule for the evolution of a PTEN-cleaving BoNT/E protease variant.

<u>PACE-E(0265)</u>				
Input phage	Phase 1 APs	Phase 2 APs	Phase 3 APs	Output phage
SP-BoNT/E NNK(E159/N161)	AP-SS.E1a	AP-SS.E1a	AP-SS.E1a	SP-E(0265)A
SP-BoNT/E NNK(E159/N161)	AP-SS.E1a	AP-SS.E1a	AP-SS.E1a	SP-E(0265)B
SP-BoNT/E NNK(H216/K225)	AP-SS.E1b	AP-SS.E1b	AP-SS.E1b	SP-E(0265)C
SP-BoNT/E NNK(H216/K225)	AP-SS.E1b	AP-SS.E1b	AP-SS.E1b	SP-E(0265)D
<u>PACE-E(0276)</u>				
Input phage	Phase 1 AP	Phase 2 AP	Phase 3 AP	Output phage
SP-E(0265)A	AP-SS.E2	AP-SS.E2	AP-SS.E2	SP-E(0276)A
SP-E(0265)B NNK(H216/K225)	AP-SS.E2	AP-SS.E2	AP-SS.E2	SP-E(0276)B
SP-E(0265)C	AP-SS.E2	AP-SS.E2	AP-SS.E2	SP-E(0276)C
SP-E(0265)D NNK(E159/H161)	AP-SS.E2	AP-SS.E2	AP-SS.E2	SP-E(0276)D
<u>PACE-E(0281)</u>				
Input phage	Phase 1 AP	Phase 2 APs	Phase 3 AP	Output phage
SP-E(0276)A	AP-SS.E3	AP-SS.E3 + AP-SS.E4	AP-SS.E4	SP-E(0281)A
SP-E(0276)B	AP-SS.E3	AP-SS.E3 + AP-SS.E4	AP-SS.E4	SP-E(0281)B
SP-E(0276)C	AP-SS.E3	AP-SS.E3 + AP-SS.E4	AP-SS.E4	SP-E(0281)C
SP-E(0276)D	AP-SS.E3	AP-SS.E3 + AP-SS.E4	AP-SS.E4	SP-E(0281)D
<u>PACE-E(0285)</u>				
Input phage	Phase 1 AP	Phase 2 APs	Phase 3 AP	Output phage
SP-E(0281)A	AP-SS.E4	AP-SS.E4 + AP-PTEN(low)	AP-PTEN(low)	SP-E(0281)A
SP-E(0281)B	AP-SS.E4	AP-SS.E4 + AP-PTEN(low)	AP-PTEN(low)	SP-E(0281)B
SP-E(0281)C	AP-SS.E4	AP-SS.E4 + AP-PTEN(low)	AP-PTEN(low)	SP-E(0281)C
SP-E(0281)D	AP-SS.E4	AP-SS.E4 + AP-PTEN(low)	AP-PTEN(low)	SP-E(0281)D
<u>PACE-E(0299)</u>				
Input phage	Phase 1 AP	Phase 2 APs	Phase 3 AP	Output phage
SP-E(0281)A	AP-PTEN(med)	AP-PTEN(med)	AP-PTEN(med)	SP-E(0281)A
SP-E(0281)B	AP-PTEN(med)	AP-PTEN(med)	AP-PTEN(med)	washout
SP-E(0281)C	AP-PTEN(med)	AP-PTEN(med)	AP-PTEN(med)	washout
SP-E(0281)D	AP-PTEN(med)	AP-PTEN(med)	AP-PTEN(med)	washout
<u>PACE-E(0308)</u>				
Input phage	Phase 1 APs	Phase 2 APs	Phase 3 AP	Output phage
SP-E(0281)A	AP-PTEN + AP _{neg} -SNAP25(T3b)	AP-PTEN + AP _{neg} -SNAP25(T3b)	AP-PTEN + AP _{neg} -SNAP25(T3b)	washout
SP-E(0281)A	AP-PTEN + AP _{neg} -SNAP25(T3a)	AP-PTEN + AP _{neg} -SNAP25(T3a)	AP-PTEN + AP _{neg} -SNAP25(T3a)	SP-E(0285)B

Table S9. E(4130) genotypes after the final PANCE passages at high selection stringency from three replicates. Mutations in red boxes were not observed prior to negative selection.

Position	26	27	28	35	49	56	65	79	99	101	118	156	159	161	162	163	166	172	203	232	242	244	248	262	263	313	316	353	354	355	357	359	365	367	390	403	404
wild type	C	Q	E	I	G	H	D	E	S	G	N	D	E	N	S	S	S	M	I	I	T	R	N	I	I	A	I	G	Q	Y	Y	K	N	S	N	G	L
A.1	C	H	E	I	G	H	D	E	A	S	D	D	L	Y	Q	R	S	K	I	T	T	R	N	I	I	A	I	G	R	Y	Y	K	N	S	N	G	*
A.2	Y	H	E	I	G	H	D	E	A	S	D	N	L	Y	Q	R	S	K	I	T	T	R	K	I	I	A	I	G	R	P	F	K	N	S	N	G	L
A.3	Y	H	E	I	G	H	D	E	A	S	D	N	L	Y	Q	R	S	K	I	T	T	R	K	T	I	A	I	G	W	Y	F	K	N	S	D	G	L
A.4	C	H	E	I	G	H	D	E	A	S	D	D	L	Y	Q	R	S	K	I	T	T	R	K	I	I	A	I	E	R	P	F	K	N	S	N	G	L
A.5	C	H	E	I	G	H	D	E	A	S	D	D	L	Y	Q	R	S	K	I	T	T	R	K	I	I	A	I	G	W	P	F	K	N	S	D	G	L
A.6	Y	H	E	I	G	H	G	E	A	S	D	N	L	Y	Q	R	S	K	I	T	T	R	K	I	I	A	I	G	R	P	F	K	N	S	N	G	*
A.7	C	H	E	I	G	H	D	E	A	S	D	N	L	Y	Q	R	S	K	I	T	T	R	K	I	I	A	T	G	W	Y	F	K	N	S	N	G	L
A.8	C	H	E	I	G	H	D	E	T	S	D	N	L	Y	Q	R	S	K	I	T	A	R	K	I	I	A	I	G	R	P	F	K	N	S	N	G	L
B.2	Y	H	E	I	G	H	D	E	A	S	D	N	L	Y	Q	R	R	K	I	T	T	R	K	I	V	A	I	G	R	P	F	K	N	F	N	G	L
B.3	Y	H	E	I	G	H	D	E	A	S	D	N	L	Y	Q	R	S	K	I	T	T	V	K	I	I	A	I	G	R	P	F	R	N	S	N	G	L
B.4	Y	H	E	I	G	H	D	D	A	S	D	N	L	Y	Q	R	S	K	V	T	T	R	K	I	I	A	I	G	R	H	F	K	N	S	N	G	L
B.5	Y	H	E	I	G	H	D	E	A	S	D	N	L	Y	Q	R	S	K	I	T	T	R	K	I	I	A	I	G	R	P	F	K	N	S	N	G	L
B.6	Y	H	K	I	G	L	D	E	A	S	D	N	L	Y	Q	R	S	K	I	T	T	R	K	I	I	A	I	G	R	P	F	K	N	S	N	G	*
B.8	Y	H	E	I	G	L	D	E	A	S	D	N	L	Y	Q	R	S	K	I	T	T	R	K	I	I	A	I	G	R	P	F	K	N	S	N	G	L
C.1	C	H	E	I	G	H	D	E	A	S	D	N	L	Y	Q	R	S	K	I	T	T	R	K	I	I	A	I	G	R	P	F	K	N	S	N	G	*
C.2	Y	H	E	I	S	H	D	E	A	S	D	N	L	Y	Q	R	S	K	I	T	T	R	K	I	I	V	I	G	R	P	F	K	N	S	N	E	L
C.3	Y	H	E	I	G	H	D	E	A	S	D	N	L	Y	Q	R	S	K	I	T	T	R	K	I	I	A	I	G	R	P	F	K	N	S	N	G	L
C.4	C	H	E	I	G	Y	D	E	A	S	D	N	L	Y	Q	R	S	K	I	T	T	R	K	I	I	A	I	G	R	P	F	K	N	S	N	G	L
C.5	Y	H	E	I	G	H	D	E	A	S	D	N	L	Y	Q	R	S	K	I	T	T	R	K	I	I	A	I	G	R	P	F	K	N	S	N	G	*
C.5	C	H	E	V	G	H	D	E	A	S	D	N	L	Y	Q	R	S	K	I	T	T	R	K	I	I	A	I	G	W	P	F	K	S	S	N	G	*

Supplementary Methods

General methods. Antibiotics (Gold Biotechnology) were used at the following working concentrations: carbenicillin 50 µg/mL, spectinomycin 50 µg/mL, chloramphenicol 25 µg/mL, kanamycin 50 µg/mL, tetracycline 10 µg/mL, streptomycin 50 µg/mL. HyClone water (GE Healthcare Life Sciences) was used for PCR reactions and cloning. For all other experiments, water was purified using a MilliQ purification system (Millipore). Phusion U Hot Start DNA polymerase (Thermo Fisher Scientific) was used for all PCRs. Plasmids and SPs were cloned by USER assembly(1). Genes were obtained as synthesized gBlock gene fragments from Integrated DNA Technologies or PCR amplified directly from *E. coli* genomic DNA. Plasmids were cloned and amplified using either Mach1 (Thermo Fisher Scientific) or Turbo (New England BioLabs) cells. Unless otherwise noted, plasmid or SP DNA was amplified using the Illustra TempliPhi 100 Amplification Kit (GE Healthcare Life Sciences) prior to Sanger sequencing. SDS-PAGE analysis was performed using precast NuPAGE 4–12% Bis-Tris PAGE gels (Invitrogen). HEK293T cells were acquired from ATCC (CRL-3216). Mouse monoclonal antibodies against Syntaxin 1 (78.2), SNAP25 (71.1), VAMP2 (69.1), polyclonal rabbit antiserum against VAMP4 (Cat. No. 136002) were purchased from Synaptic Systems. Monoclonal rabbit antibody against PTEN (138G6) was purchase from Cell Signaling Technologies. Anti-FLAG mouse monoclonal antibody (M2) and anti-actin mouse monoclonal antibody (AC-15) were purchased from Sigma. Anti-HA epitope tag mouse monoclonal antibody (16B12) was purchase from BioLegend. Anti-Ykt6 was generously provided by Jesse C. Hay (University of Montana). A full list of plasmids used in this work is provided at the end of the supplementary materials.

Preparation and transformation of chemically competent cells. Strain S1030 or S2060(2) was used in all luciferase, phage propagation, and plaque assays, and in all PACE experiments. To prepare competent cells, an overnight culture was diluted 1000-fold into 50 mL of 2xYT media (United States Biologicals) supplemented with tetracycline and streptomycin and grown at 37°C with shaking at 230 RPM to OD₆₀₀ ~ 0.4-0.6. Cells were pelleted by centrifugation at 4000 g for 10 minutes at 4°C. The cell pellet was then resuspended by gentle stirring in 2 mL of ice-cold LB media (United States Biologicals). After resuspension, 2 mL of 2x TSS (LB media supplemented with 5% v/v DMSO, 10% w/v PEG 3350, and 20 mM MgCl₂) was added. The cell suspension was stirred to mix completely, and if not used directly, was aliquoted, frozen on dry ice, and stored at -80°C until use.

To transform cells, 100 µL of competent cells thawed on ice was added to a pre-chilled mixture of plasmid (2 µL each; up to 3 plasmids per transformation) in 95 µL KCM solution (100 mM KCl, 30 mM CaCl₂, and 50 mM MgCl₂ in H₂O) and stirred gently with a pipette tip. The mixture was incubated on ice for up to 10 min and heat shocked at 42°C for 90 s before 500 µL of SOC media (New England BioLabs) was added. Cells were allowed to recover at 37°C with shaking at 230 RPM for 1 h, streaked on 2xYT media + 1.5% agar (United States Biologicals) plates containing the appropriate antibiotics, and incubated at 37°C for 16-18 h.

Luciferase assay. S1030 cells were transformed with the AP(s) and CP(s) of interest as described above. Overnight cultures of single colonies grown in DRM media supplemented with maintenance antibiotics were diluted 250-fold into DRM media(3) with maintenance antibiotics and 0.5–5 µM arabinose in a 96-well deep well plate (Axygen). The plate was sealed with a porous sealing film and grown at 37°C with shaking at 230 RPM. After 3 hours, 100 µL of cells was transferred to a 96-well black-walled clear-bottomed plate (Costar), then 600 nm absorbance and luminescence were read using a Tecan Infinite M1000 Pro microplate reader or Tecan Spark plate reader. OD600-normalized luminescence values were obtained by dividing raw luminescence by background-subtracted 600 nm absorbance.

Plaque assay. S2060 cells transformed with pJC175e(4) (S2208) overnight cultures of single colonies grown in 2xYT media supplemented with maintenance antibiotics were diluted 1000-fold into fresh 2xYT media with maintenance antibiotics and grown at 37°C with shaking at 230 RPM to OD₆₀₀ ~ 0.6-0.8 before use. SP were serially diluted 50-fold (4 dilutions total) in LB media. 150 µL of cells was added to 50 µL of each phage dilution and to this 800 µL of liquid (55°C) top agar (2xYT media + 0.6% agar) supplemented with 2% Bluo-gal (Gold Biotechnology) was added and mixed by pipetting up and down once. This mixture was then immediately pipetted onto one quadrant of a quartered Petri dish already containing 2 mL of solidified bottom agar (2xYT media + 1.5% agar, no antibiotics). After solidification of the top agar, plates were incubated at 37°C for 16-18 h.

General method for phage-assisted continuous evolution. Unless otherwise noted, PACE apparatus, including host cell strains, lagoons, chemostats, and media, were all used as previously described(1, 3).

Chemically competent S2060s were transformed with AP(s) and MP6 as described above, plated on 2xYT media + 1.5% agar supplemented with 100 mM glucose (to prevent induction of mutagenesis) in addition to maintenance antibiotics, and grown at 37°C for 18-20 h. Four colonies were picked into 1 mL DRM each in a 96-well deep well plate, and this was diluted 5-fold eight times serially into DRM. The plate was sealed with a porous sealing film and grown at 37°C with shaking at 230 RPM for 16-18 h. Dilutions with OD₆₀₀ ~ 0.4-0.8 were then used to inoculate a chemostat containing 80 mL DRM. The chemostat was grown to OD₆₀₀ ~ 0.8-1.0, then continuously diluted with fresh DRM at a rate of ~1.1–1.5 chemostat volumes/h as previously described(3). The chemostat was maintained at a volume of 80-100 mL.

Experiments starting with an NNK mutagenized SP library began with a lagoon inoculum of 1–2 mL of phage library containing 10⁸–10¹⁰ pfu mL⁻¹. For all other experiments, lagoons were inoculated with 100 µl of filtered phage population from the last time point of the previous PACE experiment. In PACE experiments using mixtures of host cell cultures (see Table S7, S8), lagoons received equal influx of cell culture from two separate chemostats containing hosts bearing the respective APs for a period of 24 h. Samples (1000 µL) of the SP population were taken at indicated times from lagoon waste lines. These were centrifuged at 8000 g for 2 min, and the supernatant was passed through a 0.22 µm PVDF Ultrafree centrifugal filter (Millipore) and stored at 4°C. Lagoon titers were determined by plaque assays using S2060 cells transformed with pJC175e(4). For Sanger sequencing of lagoons, single plaques were picked and submitted to rolling circle amplification. Generally, eight plaques were picked and sequenced per lagoon.

General method for phage-assisted non-continuous evolution (PANCE). Chemically competent *E. coli* S1030 were transformed with desired AP and MP and plated on 2xYT agar containing 0.5-2% glucose (w/v). A single colony for each selection strain was grown to saturation overnight at 37°C in DRM containing appropriate antibiotics and diluted the next day 100- to 1000- fold into fresh DRM. Cultures were grown to log-phase (OD 0.3-0.6), and treated with 10mM arabinose to induce mutagenesis. Treated cultures were split into the desired number of 1 mL cultures in a 96-well plate, and inoculated with selection phage at the indicated dilution (see fig. S3, S7, S13, S20). Infected cultures were grown 12–16 h at 37°C and harvested the next day via centrifugation (2000 x g for 2 min). Supernatant containing evolved phage was isolated with optional filtration through a 0.2µm Costar spin filter (Corning) and stored at 4°C. Isolated phage were then used to infect the next passage and the process repeated for the duration of the selection. Phage titers were determined by plaque assay.

PANCE evolution of X(4130) proteases. PANCE was initiated using a population of selection phage encoding wild-type BoNT/X LC, which was mutagenized prior to initial selection by propagation

through strain S2208 containing mutagenesis plasmid (MP6), induced as in the general protocol (“mutagenic drift”). After diversification, initial selection occurred at low dilution coefficient in four separate host strains (each in triplicate) encoding a high stringency positive-selection AP activated by Ykt6 cleavage, as well as one of four negative selection APs that responded to VAMP1 cleavage at a range of stringencies. Initial PANCE passages were performed at low effective dilution per passage (100-fold). After five PANCE passages, only the lowest stringency conditions yielded surviving phage.

The populations from low-stringency passages were used to inoculate an additional 15 PANCE passages of simultaneous positive and negative selection (PANCE X(4130), Fig. 1B, fig. S3). We observed large improvements in phage fitness, with some phage populations capable of persisting even at high dilution (1,000-fold per passage) in the highest stringency negative-selection strain. To enrich the most fit variants within each lineage, we pooled phage populations from all negative-selection stringencies within each replicate (but not between replicates) at passage 11, and propagated the resulting phage through additional passages at high dilution (2,000-fold to 5,000-fold per passage) in all strains (Fig. 1B top). We isolated variants that survived the highest negative selection stringency from each of the three separate replicates.

PANCE evolution of X(5010) proteases. PANCE was initiated using a population of selection phage encoding wild-type BoNT/X LC, which was mutagenized prior to initial selection by propagation through strain S2208 containing mutagenesis plasmid (MP6), induced as in the general protocol. After diversification, we began with PANCE at low dilution (100- to 200-fold per passage) in triplicate, in four separate host strains (each in triplicate) encoding a high-stringency positive-selection AP activated by VAMP4 cleavage, as well as one of four negative selection APs that responded to VAMP1 cleavage at a range of stringencies. We initially observed phage titers drop rapidly at all stringencies in all three replicates, necessitating additional mutagenic drift at passage 5. After this re-diversification step, we began to observe phage survival at low dilution factors at the lowest negative selection stringency. Phage isolated after nine total passages converged on distinct sets of BoNT/X mutations between replicates (X(4253) populations).

We reinitiated PANCE using the same set of host strains that spanned a range of negative selection stringencies with concurrent high-stringency positive selection (PANCE X(5010)), and the partially VAMP4-selective phage. Slowly increasing the dilution factor over eight passages from 100-fold to 500-fold per passage resulted in phage survival in host strains at the highest negative selection stringency. We mixed populations within replicates after passage 9, and passaged surviving phage at high dilution (1,000- to 5,000-fold per PANCE passage) for an additional three passages (fig. S6). Clones were sequenced from the three replicates passaged in the highest stringency negative selection host cells at passage 12 (Table S3).

PANCE evolution of F(3230) proteases. PANCE was initiated using the F(3041) populations of selection phage encoding VAMP7-cleaving BoNT/F LC variants from positive selection PACE. We began with PANCE at low dilution (100- to 200-fold per passage) in duplicate high-stringency positive selection for VAMP7 cleavage with concurrent negative selection against VAMP1 cleavage at four separate negative selection stringencies (low to very high) determined by the strength of the RBS mediating translation of the gIII-neg transcript (Fig. 3A). After 2–3 alternating cycles of selection and mutagenic drift (five passages total), we increased the dilution factor for each PANCE passage from 100-fold to 200-fold, and stopped the genetic drift passages, forcing phage to propagate solely on their ability to survive positive and negative selections. Initially, phage persisted only in hosts carrying the two lowest-stringency negative selection VAMP1 APs at these modest dilution rates. We used these continuously evolving populations to periodically reinfect high-stringency negative selection host cells

(fig. S11). As the low-stringency populations continued to evolve, they eventually accessed solutions capable of surviving in high-stringency selection strains at 10-fold higher dilution levels than initial passages. After 15 total passages of dual positive and negative selection PANCE, we analyzed clones (Table S6) from the phage populations passaged in the highest stringency negative selection hosts in luciferase assays (Fig. 3C).

PANCE evolution of E(4130) proteases. We performed a total of 15 passages of simultaneous positive and negative selection PANCE in triplicate at four different negative selection stringencies, with increasing dilution levels between passages. The selectivity of the input phage was sufficient to propagate on all but the highest stringency negative selection at relatively low dilution factors (100-fold dilution per passage, fig. S18). By passage 5, phage titers at the very high-stringency negative selection had begun to recover, and the dilution rate was increased to 400-fold per passage, and then to 1,000-fold until passage 11. Phage populations from all stringencies within each replicate trajectory were mixed to allow variants to compete, and the final three passages of this PANCE campaign were performed at high dilution factors (1,000- to 5,000-fold per passage). At passage 15, the phage populations from the host cells containing the highest stringency negative selection APs, were sequenced and analyzed (Table S9).

General methods for protease expression and purification. Single colonies of *E. coli* BL21(DE3) (New England Biolabs) harboring the 6xHis-tagged protease of interest were cultured in 2xYT with kanamycin (50 ug/mL) overnight at 37 °C at 230 rpm. Overnight cultures were then back diluted 1:100 into fresh 2xYT media (250–1000 mL) supplemented with kanamycin (50 ug/mL) and grown to until $OD_{600} = 0.4–0.7$. After 1 h cold shock on ice, isopropyl- β -d-thiogalactoside (IPTG; Gold Biotechnology) was added to a final concentration of 1 mM, and the cells were induced overnight at 16 °C. The cells were pelleted by centrifugation (5 min @ 60000 x g) and resuspended in cold lysis buffer (10 mL per 250 mL culture, 20 mM HEPES pH 7.3, 200 mM NaCl, Roche cComplete EDTA-free protease inhibitor tablet), and lysed by two passages through an Avestin Emulsiflex C3 homogenizer. Lysate was clarified by high-speed centrifugation (20 min @ 19,000 x g, 4 °C) then poured onto TALON Co-affinity resin (Takara Bio), 1 mL per 250 mL culture) pre-equilibrated with cold wash buffer (20 mM HEPES pH 7.3, 200 mM NaCl) and then tumbled gently end-over-end for 1 h at 4 °C. After binding, resin was added to isolation column, and washed with cold wash buffer (20 mL + 5 mL) then eluted in six 1 mL–3 mL fractions of wash buffer supplemented with imidazole at increasing concentration (F1: 10 mM imidazole, F2: 20 mM imidazole, F3: 50 mM imidazole, F4: 100 mM imidazole, F5–F6: 250 mM imidazole). Fractions were analyzed by SDS-PAGE gel, and pure fractions were pooled, and submitted to buffer exchange by serial centrifugal concentration into wash buffer (20 mM HEPES pH 7.3, 200 mM NaCl). Protein concentration was determined by Bradford assay.

For dually-tagged proteases with C-terminal His tag and N-terminal MBP solubility tag (BoNT/F, F(3041)B6, and F(3230)A3), eluted fractions from the Co-affinity resin were pooled and submitted to buffer exchange, then diluted into 10–15 mL of wash buffer containing 1 mL of Amylose resin (New England Biolabs), and tumbled gently end-over-end at 4 °C for 1 h. Bound resin and supernatant were then poured into column, and column was washed with cold wash buffer (20 mL + 5 mL), then protease was eluted in four 1.4 mL fractions of wash buffer supplemented with 10 mM maltose (Sigma-Aldrich). Fractions were analyzed by SDS-PAGE gel, and pure fractions were pooled, and submitted to buffer exchange by serial centrifugal concentration into wash buffer (20 mM HEPES pH 7.3, 200 mM NaCl). Protein concentration was determined by Bradford assay.

General methods for FRET substrate expression and purification

Single colonies of *E. coli* BL21(DE3) (New England Biolabs) harboring the 6xHis-tagged protease of interest were cultured in 2xYT with kanamycin (50 ug/mL) overnight at 37 °C at 230 rpm. Overnight cultures were then back diluted 1:100 into fresh 2xYT media (250–1000 mL) supplemented with kanamycin (50 ug/mL) and grown to until OD₆₀₀ = 0.4–0.7. After 1 h cold shock on ice, isopropyl-β-d-thiogalactoside (IPTG; Gold Biotechnology) was added to a final concentration of 1 mM, and the cells were induced overnight at 16 °C. The cells were pelleted by centrifugation (5 min @ 60000 x g) and resuspended in cold lysis buffer (10 mL per 250 mL culture, 20 mM HEPES pH 7.3, 200 mM NaCl, Roche cOmplete EDTA-free protease inhibitor tablet), and lysed by sonication. Lysate was clarified by high-speed centrifugation (20 min @ 19,000 x g, 4 °C) then poured onto TALON Co-affinity resin (Takara Bio, 500 μL per 250 mL culture) pre-equilibrated with cold wash buffer (20 mM HEPES pH 7.3, 200 mM NaCl) and then tumbled gently end-over-end for 1 h at 4 °C. After binding, resin was added to isolation column, and washed with cold wash buffer (20 mL + 5 mL) then eluted in six 1 mL – 3 mL fractions of wash buffer supplemented with imidazole at increasing concentration (F1: 10 mM imidazole, F2: 20 mM imidazole, F3: 50 mM imidazole, F4: 100 mM imidazole, F5–F6: 250 mM imidazole). Fractions were analyzed by SDS-PAGE gel, and pure fractions were pooled, and submitted to buffer exchange by serial centrifugal concentration into wash buffer (20 mM HEPES pH 7.3, 200 mM NaCl). Protein concentration was determined by Bradford assay.

General methods for protease cleavage gel shift assays

Isolated proteases and MBP-GST fusion substrates were diluted into reaction buffer (50 mM HEPES pH 7.3, 5 mM NaCl, 0.1% Tween-80, 2 mM DTT, and 10 μM Zn(OAc)₂) to generate a 2x stock solution stock enzyme mixture on ice. Protease and substrate solutions were then mixed (1:1) and incubated at 37 °C for 1–2 hrs. Reactions were stopped by addition of TruPAGE sample buffer (Sigma Aldrich), and analyzed by SDS-PAGE gel electrophoresis.

General methods for protease kinetic measurements

Isolated proteases were diluted into reaction buffer (50 mM HEPES pH 7.3, 5 mM NaCl, 0.1% Tween-80, 2 mM DTT, and 10 μM Zn(OAc)₂) to make a 20x stock enzyme mixture and stored on ice. Separately, FRET protease substrates were diluted into reaction buffer at 1.05x the intended concentration. Substrate mixtures (47.5 μL) were then aliquoted (in triplicate) into wells of a 96-well clear-bottomed half-volume plate (Corning no. 3880) and warmed to 37 °C in the analysis chamber of a Tecan Infinite M1000 Pro microplate reader or Tecan Spark plate reader. Protease (2.5 μL of 20x stock) was then added, and assay initiated at 37 °C. Fluorescence was recorded every 60–90s for emission at both 470 nm and 526 nm wavelengths (with excitation at 434 nm) for 1 h. at 1 h, 1 μL of trypsin was added to each well, and emission endpoint (Em₄₇₀ and Em₅₂₆ for 434 nm excitation) was measured until both fluorescence measurements became stable (usually ~5–7 min). Conversion was calculated at each time point as previously reported according to the equation:

$$\text{Conversion} = [S]_0 * (X - \text{neg}) / (\text{pos} - \text{neg})$$

where [S]₀ is the initial substrate concentration, *X* is the Em₄₇₀/Em₅₂₆ at a given timepoint, *neg* is the mean Em₄₇₀/Em₅₂₆ from three replicates of protease-free substrate control at the equivalent timepoint, and *pos* is the Em₄₇₀/Em₅₂₆ ratio upon complete conversion (trypsinolysis). Data was processed using Microsoft excel and subsequently plotted and fit using PRISM GraphPad.

Crystallization, data collection, and structure determination

X(4130)B1 (residues 1–439) was subcloned into a pET28a vector with a C-terminal His₆ tag and expressed in *E. coli* strain BL21 (DE3) at 20 °C in autoinduction medium (Formedium). After cell lysis by sonication and centrifugation, the supernatant was applied to a HisTrap (GE Healthcare) nickel

column and the bound protein was eluted with a linear imidazole gradient from 20 mM to 500 mM. The protein was further purified with HiLoad 16/60 Superdex 75 (GE Healthcare) gel filtration column and then concentrated to 10 mg/mL in buffer of 200 mM NaCl, 20 mM Tris, pH 7.5. Crystallization was performed via the sitting drop vapor diffusion method at 4 °C by mixing equal volumes (0.2–1.0 μ L) of X(4130)B1 and the reservoir solution. Crystals were grown from the reservoir condition: 20% (w/v) polyethylene glycol monomethyl ether 5,000, 0.1 M Bis-Tris, pH 6.5. The crystal was briefly soaked in cryoprotectant solution containing the reservoir solution supplemented with 10% glycerol and flash-frozen in liquid nitrogen for data collection. The diffraction data set was collected at the LS-CAT beamline 21-ID-G, Advanced Photon Source (APS).

All diffraction images were indexed, integrated, and merged using HKL2000 (5). The structure was determined by molecular replacement using PHASER (6) with the BoNT/X wild-type LC structure (PDB ID: 6F47) as the search model. Structural refinement was carried out using REFMAC v.5.8.0267 (7), the water molecules were generated using ARP/wARP (8), and ligands were added to the model manually during visual inspection in COOT (9). Translation–Libration–Screw (TLS) groups were created by the TLSMD server (10) and TLS corrections were applied during the final stages of refinement. MolProbity (11) was used for monitoring the quality of the model during refinement and for the final validation of the structure. The structure was deposited to the Protein Data Bank (<https://www.rcsb.org/>) with the assigned PDB code 7KZ7. Detailed data collection and refinement statistics are summarized in Table S2. Structural figures were created using the PYMOL (<http://www.pymol.org/>) program.

Cleavage of full-length PTEN in HEK293 cells and cell viability assays

Full-length FLAG-tagged PTEN in pCDNA3.1 vectors was co-transfected with HA-tagged E(4130)A2 or PH-E(4130)A2 in HEK293 cells using PolyJet transfection reagent (SignaGen, MD) following the manufacturer's instructions. Cell lysates were harvested 24 hours later in lysis buffer (PBS with 1% Triton-X100, 0.1% SDS, pH 7.4) plus EDTA-free protease inhibitor cocktail (APExBIO, TX). The lysates were analyzed by immunoblot, detecting PTEN (using an anti-FLAG tag antibody), E(4130)A2 (using an anti-HA tag antibody), and PH-E(4130)A2 (using an anti-HA tag antibody). Actin was also detected as a loading control. For assessing cell viability, E(4130)A2, PH-E(4130)A2 or empty pCDNA3.1 vector was transfected into 293T cells at 50% confluency using PolyJet transfection reagents. The cell viability was measured 24 hours later using CCK-8 reagent (APExBIO, TX) following the manufacturer's instructions.

Cleavage of full-length VAMPs and Ykt6 in cell lysates

Full-length HA-tagged VAMP2, VAMP4, and Ykt6 were transfected into 293T cells using PolyJet transfection reagents following the manufacturer's instructions. Cell lysates were harvested 24 h later in lysis buffer (PBS with 1% Triton-X100, 0.1% SDS, pH 7.4) with EDTA-free protease inhibitor cocktail (APExBIO, TX). Cell lysates (12 μ L) were incubated with serial dilutions of wild-type, X(4130)B1, or X(5010)B1 proteases at 37 °C (30 min for VAMP substrates and 1 h for Ykt6). Samples were analyzed by immunoblot using an anti-HA tag antibody.

Sortase-mediated ligation

His6-HA-H_C/A was cleaved overnight at 4 °C using thrombin before being added into the ligation reaction mixture. Ligation reaction was set up in 50 μ L TBS buffer with LC-H_N (4 μ M), H_C/A (4 μ M), Ca²⁺ (10 mM) and sortase (0.5 μ M), for 40 min at room temperature. An aliquot of the ligation mixture (7.5 μ L) was analyzed on 10% SDS-PAGE. The rest of ligation mixture was then incubated with 10 μ L Ni-NTA Sepharose beads on ice for 10 min. The supernatant was transferred to a new tube and incubate with thrombin (0.4 U) for 30 min at room temperature. An aliquot of thrombin activated

toxin was analyzed on SDS-PAGE together with bovine serum albumin (BSA) standard for quantification.

Neuron culture and immunoblot analysis

Primary rat cortical neurons were prepared from embryonic day 18 (E18) to E19 embryos (Sprague-Dawley rat) using a papain dissociation kit (Worthington Biochemical, NJ) following the manufacturer's instruction. Neurons (10 days in culture) were exposed to ligated chimeric toxins containing wild-type BoNT/X LC, X(4130)B1, or X(5010)B1 in culture medium for 16 h. Cell lysates were harvested in lysis buffer (PBS with 1% Triton-X100, 0.1% SDS, pH 7.4) plus EDTA-free protease inhibitor cocktail (APExBIO, TX). Lysates were subjected to SDS-PAGE and immunoblot analysis, detecting endogenous VAMP2, VAMP4, and Ykt6 using their respective antibodies.

Lentivirus production and cultured neuron infection

The packing plasmid psPAX2 (15 μ g), envelope plasmid pCI-VSVG (2.5 μ g) together with the plasmid Syn-lox encoding RFP, or PH-E(4130)A2 were transfected into HEK293T growing in 15-cm culture dishes. The lentiviral particles in the supernatant were spun down by ultracentrifuge (20,000 rpm, 2 h), resuspended in PBS, aliquoted, and stored in -80 °C. Rat cortical neurons were infected on day 5 in culture, harvested, and lysed 7 days after infection using lysis buffer (PBS with 1% Triton-X100, 0.1% SDS, pH 7.4) with EDTA-free protease inhibitor cocktail (APExBIO, TX). Neuron lysates were analyzed by immunoblot detecting endogenous PTEN, SNAP-25, VAMP2, and Syntaxin 1.

Plasmids used in this study

Name	Class (res)	Origin	ORF1		ORF2	
			Promoter	[RBS] Genes	Promoter	[RBS] Genes
pJC175e	AP (carb ^R)	SC101	P _{psp}	[sd7] gIII, luxAB		
AP-SNAP25	AP (carb ^R)	SC101	P _{T7}	[sd7] gIII, luxAB	P _{ProB}	[sd8] SNAP25-T7PAP
AP-VAMP1	AP (carb ^R)	SC101	P _{T7}	[sd7] gIII, luxAB	P _{ProB}	[sd7] VAMP1(T29-K89)-T7PAP
AP-Ykt6	AP (carb ^R)	SC101	P _{T7}	[sd7] gIII, luxAB	P _{ProB}	[sd7] Ykt6(L161-L177)-T7PAP
AP-SS.F1	AP (carb ^R)	SC101	P _{T7}	[sd7] gIII, luxAB	P _{ProB}	[sd7] SS.F1-T7PAP
AP-SS.F2	AP (carb ^R)	SC101	P _{T7}	[sd7] gIII, luxAB	P _{ProB}	[sd7] SS.F2-T7PAP
AP-SS.F3	AP (carb ^R)	SC101	P _{T7}	[sd7] gIII, luxAB	P _{ProB}	[sd7] SS.F3-T7PAP
AP-SS.F4	AP (carb ^R)	SC101	P _{T7}	[sd7] gIII, luxAB	P _{ProB}	[sd7] SS.F4-T7PAP
AP-SS.F7	AP (carb ^R)	SC101	P _{T7}	[sd7] gIII, luxAB	P _{ProB}	[sd7] SS.F7-T7PAP
AP-VAMP7(low)	AP (carb ^R)	SC101	P _{T7}	[sd7] gIII, luxAB	P _{ProB}	[sd7] VAMP7(K121-R180)-T7PAP
AP-VAMP7(high)	AP (carb ^R)	SC101	P _{T7(A12C)}	[sd4] gIII, luxAB	P _{ProB}	[sd7] VAMP7(K121-R180)-T7PAP(Q649S)
AP-VAMP1(X)	AP (carb ^R)	SC101	P _{T7}	[sd7] gIII, luxAB	P _{ProB}	[sd7] VAMP1(L56-L72)-T7PAP
AP-VAMP4	AP (carb ^R)	SC101	P _{T7}	[sd7] gIII, luxAB	P _{ProB}	[sd7] VAMP4(I75-L91)-T7PAP
AP-VAMP5	AP (carb ^R)	SC101	P _{T7}	[sd7] gIII, luxAB	P _{ProB}	[sd7] VAMP5(L28-L44)-T7PAP
AP _{T3} -VAMP1	AP (carb ^R)	SC101	P _{T3}	[sd4] gIII, luxAB	P _{ProB}	[sd9] VAMP1-T3'PAP
AP _{T3} -VAMP7	AP (carb ^R)	SC101	P _{T3}	[sd4] gIII, luxAB	P _{ProB}	[sd9] VAMP7-T3'PAP
AP _{T3} -Ykt6	AP (carb ^R)	SC101	P _{T3}	[sd4] gIII, luxAB	P _{ProB}	[sd9] Ykt6(L161-L177)-T3'PAP
AP _{T3} -VAMP4	AP (carb ^R)	SC101	P _{T3}	[sd4] gIII, luxAB	P _{ProB}	[sd9] VAMP4(I75-L91)-T3'PAP
AP-SS.E1a	AP (carb ^R)	SC101	P _{T7}	[sd7] gIII, luxAB	P _{ProC}	[sd8] SS.E1a-T7PAP
AP-SS.E1b	AP (carb ^R)	SC101	P _{T7}	[sd7] gIII, luxAB	P _{ProC}	[sd8] SS.E1b-T7PAP
AP-SS.E2	AP (carb ^R)	SC101	P _{T7}	[sd7] gIII, luxAB	P _{ProC}	[sd8] SS.E2-T7PAP
AP-SS.E3	AP (carb ^R)	SC101	P _{T7}	[sd7] gIII, luxAB	P _{ProC}	[sd8] SS.E3-T7PAP
AP-SS.E4	AP (carb ^R)	SC101	P _{T7}	[sd7] gIII, luxAB	P _{ProC}	[sd8] SS.E4-T7PAP
AP-PTEN(low)	AP (carb ^R)	SC101	P _{T7}	[sd7] gIII, luxAB	P _{ProC}	[sd8] PTEN-T7PAP
AP-PTEN(med)	AP (carb ^R)	SC101	P _{T7}	[sd7] gIII, luxAB	P _{ProB}	[sd8] PTEN-T7PAP
AP _{T3} -PTEN (PTEN med/high)	AP (carb ^R)	SC101	P _{T3}	[sd4] gIII, luxAB	P _{ProC}	[sd9] PTEN-T3'PAP
AP _{T3} -PTEN (PTEN high)	AP (carb ^R)	SC101	P _{T3}	[sd4] gIII, luxAB	P _{ProB}	[sd9] PTEN-T3'PAP
AP _{T3} -PTEN (PTEN v. high)	AP (carb ^R)	SC101	P _{T3}	[sd4] gIII, luxAB	P _{ProA}	[sd9] PTEN-T3'PAP
AP _{neg} -VAMP1a	AP-neg (spec ^R)	p15a	P _{T7}	[sd7] gIII-neg, luxAB	P _{ProD}	[sd8] VAMP1(T29-K89)-T7PAP
AP _{neg} -VAMP1b	AP-neg (spec ^R)	p15a	P _{T7}	[sd4] gIII-neg, luxAB	P _{ProD}	[sd8] VAMP1(T29-K89)-T7PAP
AP _{neg} -VAMP1c	AP-neg (spec ^R)	p15a	P _{T7}	[sd2] gIII-neg, luxAB	P _{ProD}	[sd8] VAMP1(T29-K89)-T7PAP
AP _{neg} -VAMP1d	AP-neg (spec ^R)	p15a	P _{T7}	[sd4U] gIII-neg, luxAB	P _{ProD}	[sd8] VAMP1(T29-K89)-T7PAP
AP _{neg} -SNAP25(T3a)	AP-neg (spec ^R)	p15a	P _{T3}	[sd4U] gIII-neg, luxAB	P _{ProA}	[sd8] SNAP25-T3'PAP
AP _{neg} -SNAP25(T3b)	AP-neg (spec ^R)	p15a	P _{T3}	[sd4U] gIII-neg, luxAB	P _{ProB}	[sd8] SNAP25-T3'PAP
AP _{neg} -SNAP25a	AP-neg (spec ^R)	p15a	P _{T7}	[sd7] gIII-neg, luxAB	P _{ProD}	[sd8] SNAP25-T7PAP
AP _{neg} -SNAP25b	AP-neg (spec ^R)	p15a	P _{T7}	[sd4] gIII-neg, luxAB	P _{ProD}	[sd8] SNAP25-T7PAP
AP _{neg} -SNAP25c	AP-neg (spec ^R)	p15a	P _{T7}	[sd2] gIII-neg, luxAB	P _{ProD}	[sd8] SNAP25-T7PAP
AP _{neg} -SNAP25d	AP-neg (spec ^R)	p15a	P _{T7}	[sd4U] gIII-neg, luxAB	P _{ProD}	[sd8] SNAP25-T7PAP
pET-mBoNT/F	EP (kan ^R)	pBR322	P _{T7lac}	MBP-BoNT/F-LC(1-428)-6xHis		
pET-mF(3041)B6	EP (kan ^R)	pBR322	P _{T7lac}	MBP-F(3041)B6-6xHis		
pET-mF(3230)A3	EP (kan ^R)	pBR322	P _{T7lac}	MBP-F(3230)A3-6xHis		
pET-BoNT/X	EP (kan ^R)	pBR322	P _{T7lac}	BoNT/X-LC(1-439)-6xHis		
pET-X(4130)B1	EP (kan ^R)	pBR322	P _{T7lac}	X(4130)B1-6xHis		
pET-X(5010)B1	EP (kan ^R)	pBR322	P _{T7lac}	X(5010)B1-6xHis		
pET-BoNT/E	EP (kan ^R)	pBR322	P _{T7lac}	BoNT/E-LC(1-411)-6xHis		
pET-E(0285)B6	EP (kan ^R)	pBR322	P _{T7lac}	E(0285)B6-6xHis		
pET-E(4130)A2	EP (kan ^R)	pBR322	P _{T7lac}	E(4130)A2-6xHis		
pET-CV-VAMP1	EP (kan ^R)	pBR322	P _{T7lac}	eCFP-VAMP1(T29-K89)-mVenus		
pET-CV-VAMP2	EP (kan ^R)	pBR322	P _{T7lac}	eCFP-VAMP2(T27-R86)-mVenus		
pET-CV-VAMP3	EP (kan ^R)	pBR322	P _{T7lac}	eCFP-VAMP3(G10-R69)-mVenus		
pET-CV-VAMP4	EP (kan ^R)	pBR322	P _{T7lac}	eCFP-VAMP4(P48-R107)-mVenus		
pET-CV-VAMP5	EP (kan ^R)	pBR322	P _{T7lac}	eCFP-VAMP5(M1-Q60)-mVenus		
pET-CV-VAMP7	EP (kan ^R)	pBR322	P _{T7lac}	eCFP-VAMP7(K121-R180)-mVenus		
pET-CVm-VAMP8	EP (kan ^R)	pBR322	P _{T7lac}	eCFP-VAMP8(G7-R67)-mVenus		
pET-CVm-Sec22b	EP (kan ^R)	pBR322	P _{T7lac}	eCFP-Sec22b(A131-H190)-mVenus		
pET-CV-Ykt6	EP (kan ^R)	pBR322	P _{T7lac}	eCFP-Ykt6(Q131-K190)-mVenus		
pET-CV-SNAP25	EP (kan ^R)	pBR322	P _{T7lac}	eCFP-SNAP25(A141-G206)-mVenus		
pET-CVm-PTEN	EP (kan ^R)	pBR322	P _{T7lac}	eCFP-PTEN(M265-N329)-mVenus		
pET-CV-VAMP1(E64L)	EP (kan ^R)	pBR322	P _{T7lac}	eCFP-VAMP1(E64L)-mVenus		
pET-CV-VAMP1(D66I)	EP (kan ^R)	pBR322	P _{T7lac}	eCFP-VAMP1(D66I)-mVenus		
pET-CV-VAMP1(A69T)	EP (kan ^R)	pBR322	P _{T7lac}	eCFP-VAMP1(A69T)-mVenus		
pET-CV-VAMP1(A71N)	EP (kan ^R)	pBR322	P _{T7lac}	eCFP-VAMP1(A71N)-mVenus		
pET-CV-VAMP1(LITN)	EP (kan ^R)	pBR322	P _{T7lac}	eCFP-VAMP1(E64L/D66I/A69T/A71N)-mVenus		
pET-MG-VAMP1	EP (kan ^R)	pBR322	P _{T7lac}	MBP-VAMP1(T29-K89)-GST		

pET-MG-VAMP7	EP (kan ^R)	pBR322	P _{T7lac}	MBP-VAMP7(K121-R180)-GST
pET-MG-SNAP25	EP (kan ^R)	pBR322	P _{T7lac}	MBP-VAMP1(M167-D186)-GST
pET-MG-PTEN	EP (kan ^R)	pBR322	P _{T7lac}	MBP-VAMP1(N292-N311)-GST
pET-CV-VAMP1(LITN)	EP (kan ^R)	pBR322	P _{T7lac}	eCFP-VAMP1(E64L/D66I/A69T/A71N)-mVenus
pBAD-BoNT/F	EV (spec ^R)	ColE1	pBAD	BoNT/F-LC(1-428)-6xHis
pBAD-dBoNT/F	EV (spec ^R)	ColE1	pBAD	BoNT/F-LC(E228Q)-6xHis
pBAD-BoNTX	EV (spec ^R)	ColE1	pBAD	BoNT/X-LC(1-439)-6xHis
pBAD-BoNT/E	EV (spec ^R)	ColE1	pBAD	BoNT/E-LC(1-411)-6xHis
pBAD-F(2020)B1	EV (spec ^R)	ColE1	pBAD	F(2020)B1-6xHis
pBAD-F(3041)B6	EV (spec ^R)	ColE1	pBAD	F(3041)B6-6xHis
pBAD-F(3230)A3	EV (spec ^R)	ColE1	pBAD	F(3230)A3-6xHis
pBAD-X(3206)A14	EV (spec ^R)	ColE1	pBAD	X(3206)A14-6xHis
pBAD-X(4130)A2	EV (spec ^R)	ColE1	pBAD	X(4130)A2-6xHis
pBAD-X(4130)B1	EV (spec ^R)	ColE1	pBAD	X(4130)B1-6xHis
pBAD-X(5010)A3	EV (spec ^R)	ColE1	pBAD	X(5010)A3-6xHis
pBAD-X(5010)B1	EV (spec ^R)	ColE1	pBAD	X(5010)B1-6xHis
pBAD-X(5010)C1	EV (spec ^R)	ColE1	pBAD	X(5010)C1-6xHis
pBAD-E(0285)B6	EV (spec ^R)	ColE1	pBAD	E(0285)B6-6xHis
pBAD-E(0308)B2	EV (spec ^R)	ColE1	pBAD	E(0308)B6-6xHis
pBAD-E(4130)A2	EV (spec ^R)	ColE1	pBAD	E(4130)A2-6xHis
pBAD-F(3230)A3-L69S	EV (spec ^R)	ColE1	pBAD	F(3230)A3-L69S-6xHis
pBAD-F(3230)A3-H72Y	EV (spec ^R)	ColE1	pBAD	F(3230)A3-H72Y-6xHis
pBAD-F(3230)A3-A106V	EV (spec ^R)	ColE1	pBAD	F(3230)A3-A106V-6xHis
pBAD-F(3230)A3-N148S	EV (spec ^R)	ColE1	pBAD	F(3230)A3-N148S-6xHis
pBAD-F(3230)A3-V150I	EV (spec ^R)	ColE1	pBAD	F(3230)A3-V150I-6xHis
pBAD-F(3230)A3-P158A	EV (spec ^R)	ColE1	pBAD	F(3230)A3-P158A-6xHis
pBAD-F(3230)A3-Y166S	EV (spec ^R)	ColE1	pBAD	F(3230)A3-Y166S-6xHis
pBAD-F(3230)A3-I167S	EV (spec ^R)	ColE1	pBAD	F(3230)A3-I167S-6xHis
pBAD-F(3230)A3-D177G	EV (spec ^R)	ColE1	pBAD	F(3230)A3-D177G-6xHis
pBAD-F(3230)A3-H184N	EV (spec ^R)	ColE1	pBAD	F(3230)A3-H184N-6xHis
pBAD-F(3230)A3-G200E	EV (spec ^R)	ColE1	pBAD	F(3230)A3-G200E-6xHis
pBAD-F(3230)A3-S224I	EV (spec ^R)	ColE1	pBAD	F(3230)A3-S224I-6xHis
pBAD-F(3230)A3-S232A	EV (spec ^R)	ColE1	pBAD	F(3230)A3-S232A-6xHis
pBAD-F(3230)A3-L240R	EV (spec ^R)	ColE1	pBAD	F(3230)A3-L240R-6xHis
pBAD-F(3230)A3-G350S	EV (spec ^R)	ColE1	pBAD	F(3230)A3-G350S-6xHis
pBAD-F(3230)A3-L360F	EV (spec ^R)	ColE1	pBAD	F(3230)A3-L360F-6xHis
pBAD-F(3230)A3-N372Y	EV (spec ^R)	ColE1	pBAD	F(3230)A3-N372Y-6xHis
pBAD-F(3230)A3-M381L	EV (spec ^R)	ColE1	pBAD	F(3230)A3-M381L-6xHis
pBAD-F(3230)A3-H396N	EV (spec ^R)	ColE1	pBAD	F(3230)A3-H396N-6xHis
pBAD-F(3230)A3-L410P	EV (spec ^R)	ColE1	pBAD	F(3230)A3-L410P-6xHis
pBAD-F(3230)A3-C-terminus	EV (spec ^R)	ColE1	pBAD	F(3230)A3-C-Terminus-6xHis
pBAD-F(3230)A3-S232A/G350S/M381L/L410P	EV (spec ^R)	ColE1	pBAD	F(3230)A3-S232A/G350S/M381L/L410P-6xHis
pBAD-E(4130)A2-Y26C	EV (spec ^R)	ColE1	pBAD	E(4130)A2-Y26C-6xHis
pBAD-E(4130)A2-H27Q	EV (spec ^R)	ColE1	pBAD	E(4130)A2-H27Q-6xHis
pBAD-E(4130)A2-A99S	EV (spec ^R)	ColE1	pBAD	E(4130)A2-A99S-6xHis
pBAD-E(4130)A2-S101G	EV (spec ^R)	ColE1	pBAD	E(4130)A2-S101G-6xHis
pBAD-E(4130)A2-D118N	EV (spec ^R)	ColE1	pBAD	E(4130)A2-D118N-6xHis
pBAD-E(4130)A2-N156D	EV (spec ^R)	ColE1	pBAD	E(4130)A2-N156D-6xHis
pBAD-E(4130)A2-L159E	EV (spec ^R)	ColE1	pBAD	E(4130)A2-L159E-6xHis
pBAD-E(4130)A2-Y161N	EV (spec ^R)	ColE1	pBAD	E(4130)A2-Y161N-6xHis
pBAD-E(4130)A2-Q162S	EV (spec ^R)	ColE1	pBAD	E(4130)A2-Q162S-6xHis
pBAD-E(4130)A2-R163S	EV (spec ^R)	ColE1	pBAD	E(4130)A2-R163S-6xHis
pBAD-E(4130)A2-K172M	EV (spec ^R)	ColE1	pBAD	E(4130)A2-K172M-6xHis
pBAD-E(4130)A2-T232I	EV (spec ^R)	ColE1	pBAD	E(4130)A2-T232I-6xHis
pBAD-E(4130)A2-K248N	EV (spec ^R)	ColE1	pBAD	E(4130)A2-K248N-6xHis
pBAD-E(4130)A2-R354Q	EV (spec ^R)	ColE1	pBAD	E(4130)A2-R354Q-6xHis
pBAD-E(4130)A2-P355Y	EV (spec ^R)	ColE1	pBAD	E(4130)A2-P355Y-6xHis
pBAD-E(4130)A2-F357Y	EV (spec ^R)	ColE1	pBAD	E(4130)A2-F357Y-6xHis
pBAD-X(4130)B1-D143N	EV (spec ^R)	ColE1	pBAD	X(4130)B1-D143N-6xHis
pBAD-X(4130)B1-T148N	EV (spec ^R)	ColE1	pBAD	X(4130)B1-T148N-6xHis
pBAD-X(4130)B1-E166A	EV (spec ^R)	ColE1	pBAD	X(4130)B1-E166A-6xHis
pBAD-X(4130)B1-I167T	EV (spec ^R)	ColE1	pBAD	X(4130)B1-I167T-6xHis
pBAD-X(4130)B1-E166A/I167T	EV (spec ^R)	ColE1	pBAD	X(4130)B1-E166A/I167T-6xHis
pBAD-X(4130)B1-N314Y	EV (spec ^R)	ColE1	pBAD	X(4130)B1-N314Y-6xHis
pBAD-X(4130)B1-I364L	EV (spec ^R)	ColE1	pBAD	X(4130)B1-I364L-6xHis

Supplementary References

1. A. H. Badran *et al.*, Continuous evolution of *Bacillus thuringiensis* toxins overcomes insect resistance. *Nature* **533**, 58-63 (2016).
2. B. P. Hubbard *et al.*, Continuous directed evolution of DNA-binding proteins to improve TALEN specificity. *Nature methods* **12**, 939-942 (2015).
3. K. M. Esvelt, J. C. Carlson, D. R. Liu, A system for the continuous directed evolution of biomolecules. *Nature* **472**, 499-503 (2011).
4. J. C. Carlson, A. H. Badran, D. A. Guggiana-Nilo, D. R. Liu, Negative selection and stringency modulation in phage-assisted continuous evolution. *Nature chemical biology* **10**, 216-222 (2014).
5. Z. Otwinowski, W. Minor, Processing of X-ray Diffraction Data Collected in Oscillation Mode. *Methods in enzymology* **276**, 307-326 (1997).
6. W. Minor, M. Cymborowski, Z. Otwinowski, M. Chruszcz, HKL-3000: the integration of data reduction and structure solution--from diffraction images to an initial model in minutes. *Acta Crystallogr D Biol Crystallogr* **62**, 859-866 (2006).
7. G. N. Murshudov *et al.*, REFMAC5 for the refinement of macromolecular crystal structures. *Acta Crystallogr D Biol Crystallogr* **67**, 355-367 (2011).
8. R. J. Morris, A. Perrakis, V. S. Lamzin, ARP/wARP and automatic interpretation of protein electron density maps. *Methods Enzymol* **374**, 229-244 (2003).
9. P. Emsley, K. Cowtan, Coot: model-building tools for molecular graphics. *Acta Crystallogr D Biol Crystallogr* **60**, 2126-2132 (2004).
10. J. Painter, E. A. Merritt, Optimal description of a protein structure in terms of multiple groups undergoing TLS motion. *Acta Crystallogr D Biol Crystallogr* **62**, 439-450 (2006).
11. V. B. Chen *et al.*, MolProbity: all-atom structure validation for macromolecular crystallography. *Acta Crystallogr D Biol Crystallogr* **66**, 12-21 (2010).